Available online at www.sciencedirect.com

SCIENCE DIRECT®

PALAEO

ELSEVIER

Palaeogeography, Palaeoclimatology, Palaeoecology 216 (2005) 73–97

www.elsevier.com/locate/palaeo

High-resolution palynological analysis in late early–middle Miocene core from the Pannonian Basin, Hungary: climatic changes, astronomical forcing and eustatic fluctuations in the Central Paratethys

Gonzalo Jiménez-Moreno[a,b,*], Francisco J. Rodríguez-Tovar[a], Eulogio Pardo-Igúzquiza[c], Séverine Fauquette[d], Jean-Pierre Suc[b], Pál Müller[e]

[a]*Laboratoire Paléoenvironnements et PaléoBiosphère (UMR CNRS 5125), Université Claude Bernard-Lyon 1, 27-43 boulevard du 11 Novembre, 69622 Villeurbanne, France*

[b]*Departamento de Estratigrafía y Paleontología, Universidad de Granada, Avda. Fuente Nueva S/N 18002, Granada, Spain*

[c]*Departamento de Geodinámica, Universidad de Granada, Avda. Fuente Nueva S/N 18002, Granada, Spain*

[d]*Institut des Sciences de l'Evolution de Montpellier, Equipe Paléoenvironnements (UMR CNRS 5554), Université Montpellier 2 (case postale 061), Place Eugène Bataillon, 34095 Montpellier, France*

[e]*Geological Institute of Hungary, Földtani Intézet, Stefánia t.14, 1143, Budapest, Hungary*

Abstract

High-resolution palynological analysis in the Karpatian–Sarmatian (late early–middle Miocene) interval of the borehole Tengelic 2 (Hungary) reveals the existence of a forest organized in altitudinal belts developed in a subtropical–warm temperate humid climate, reflecting the so-called Miocene climatic optimum. Pollen changes from the late early Miocene to the middle Miocene are related to climatic variations. Values of mean annual temperature (Ta) between 18 and 20 °C and mean annual precipitation (Pa) between 1200 and 1400 mm have been estimated ("climatic amplitude method") for the Badenian. Decreasing during Late Badenian and Sarmatian, Ta and Pa about 16 °C and 1100 mm, have been interpreted as a climatic cooling correlated with the "Monterey cooling event" and related to the development of the East Antarctic Ice Sheet (EAIS). Alternation in pollen taxa (thermophilous vs. altitudinal elements) reflects the astronomical forcing on temperature and precipitation and then on vegetation, where obliquity and eccentricity cycles dominated. Eustatic changes determine *Pinus* and Pinaceae and dinocyst variations.

Keywords: Palynology; Climatic quantification; Cyclostratigraphy; Eustatic changes; Early–middle Miocene; Pannonian Basin

* Corresponding author. Departamento de Estratigrafía y Paleontología, Universidad de Granada, Avda. Fuente Nueva S/N 18002, Granada, Spain. Tel.: +34 958243347; fax: +34 958248528.

E-mail address: gonzaloj@ugr.es (G. Jiménez-Moreno).

0031-0182/$ - see front matter © 2004 Elsevier B.V. All rights reserved.
doi:10.1016/j.palaeo.2004.10.007

1. Introduction

Palynology studies dealing with Miocene sediments in Europe have been carried out from the late 1960s to present, improving knowledge of vegetation and climate during this time in the European area (Naud and Suc, 1975; Suc and Bessedik, 1981; Bessedik, 1985; Zheng, 1990; Rivas-Carballo, 1991; Valle et al., 1995; Bertini et al., 1998; Barrón, 1999; Ivanov et al., 2002). Some of these articles focused on Miocene palynology in the Pannonian Basin (Planderová, 1990; Nagy, 1991, 1992), but methodological aspects, such as morphologic taxonomy and the lack of any quantitative information, are debatable. Palynological studies have been carried out with a cyclostratigraphy goal (i.e., in the continental early Pliocene of Romania; Popescu, 2001; Popescu et al., in press) but never focusing on the middle Miocene or dealing with marine sediments.

The aim of this article is to reconstruct and interpret the developed vegetation in the late early and middle Miocene surrounding the Pannonian Basin (Hungary) based on a high-resolution pollen analysis of the borehole Tengelic 2 using botanical taxonomy and a quantitative approach to the pollen data. Palynological information allows for paleoenvironmental reconstructions to determine the influence of astronomical climatic changes and eustatic fluctuations in the origin and evolution of the studied vegetation. Dinoflagellate cysts are abundant in the samples and have been studied as well to improve the obtained information.

2. Regional setting

The 1183-m-thick borehole Tengelic 2 is located in the Pannonian Basin in southern Hungary (46° 31′ 59.9″ N, 18° 43′ E; Fig. 1).

The Pannonian Basin, a back-arc basin type, was formed during the Neogene in eastern-central Europe as a consequence of the African–Eurasian convergence. It occupied what is now Hungary, Slovakia, Croatia and Romania (Royden and Horváth, 1988; Fig. 2). The Pannonian Basin consisted of several subbasins in which, in some cases, more than 5000 m of Neogene sediments was deposited (Fig. 2).

This basin, as the rest of the so-called basins of the "Paratethys," displayed during the Neogene a long-

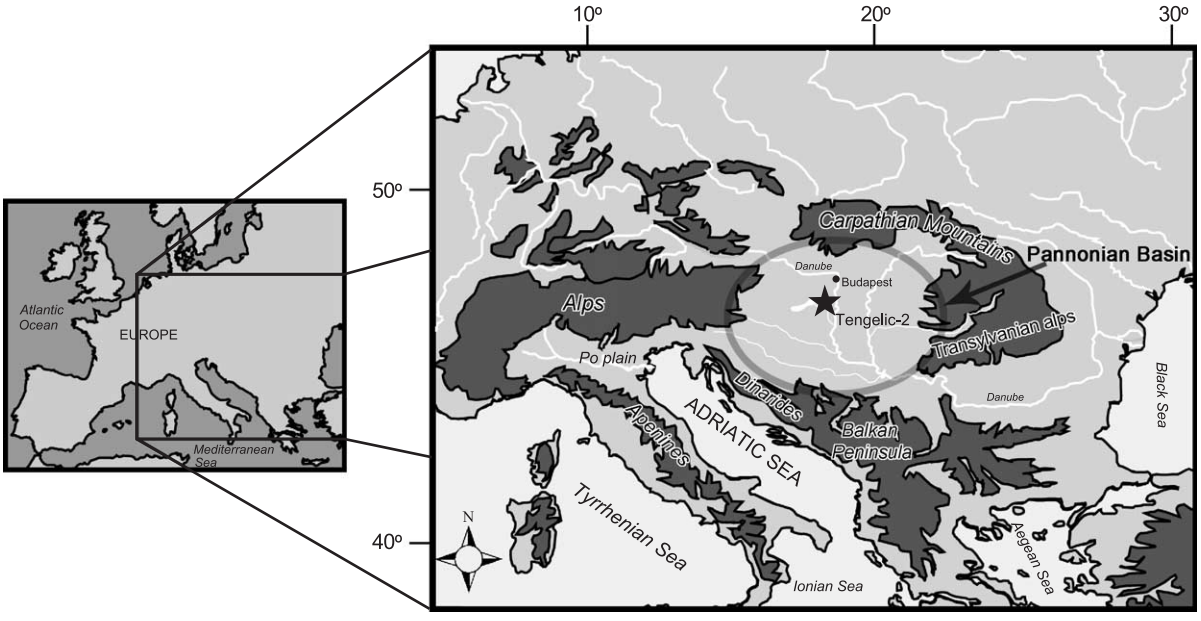

Fig. 1. Location of the borehole Tengelic 2 within the Pannonian Basin. The main reliefs of this region.

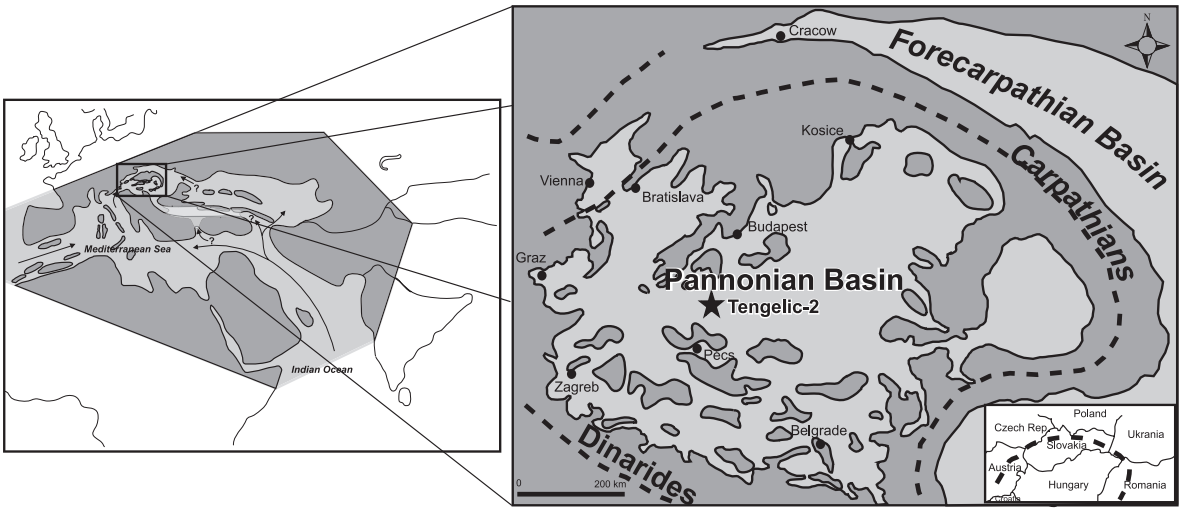

Fig. 2. Paleogeographic map of the Pannonian Basin during the Badenian (middle Miocene) after Hámor (1995) and Rögl (1998). Location of the Tengelic 2 borehole.

term trend of decreasing marine influence and a correlative reduction in size with regard to the marine depositional domains. During the Karpatian (late early Miocene), this area was characterized by the presence of large alluvial fans and lakes, and as a result, continental sediments were deposited (Tari, 1992). These sediments are interfingered with a volcanic tuff, which probably reflects the influence of very active tectonics at that time. Later on, during the Early Badenian (early middle Miocene), the sediments of the studied area reflect the progressive transition from continental to brackish and then to marine conditions. The area was then occupied mainly by a shallow sea which evolved into a more restricted sea in the Sarmatian (late middle Miocene), and then at the Sarmatian–Pannonian boundary (Serravallian–Tortonian boundary), the Central Paratethys became entirely restricted, and the brackish Lake Pannon established (Hámor, 1995; Rögl, 1998; Meulenkamp and Sissingh, 2003).

3. Materials and methods

3.1. Borehole Tengelic-2

Sediments from Karpatian, Badenian and Sarmatian ages are well represented in the studied borehole Tengelic 2 (Bohn-Havas, 1982; Korecz-Laky, 1982; Nagymarosi, 1982; Fig. 3). The Karpatian and part of the Early Badenian are mainly characterized by terrigenous effusive vulcanites, the Tar Dacite tuff, which are intercalated by some layers of lacustrine–brackish sediments or even marine sediments (deduced by the presence of marine dinocysts). The volcanic sediments have been dated, the youngest (872 m core depth) being 16±0.7 Ma in age (Hálmai et al., 1982). They are covered by dark clays rich in organic mater and later on by marine sand and silty clayey marls. Early Badenian (851–823 m) is present here but very condensed. The Late Badenian (823–723 m) is characterized by homogeneous dark clayey sediments deposited under marine shallow water conditions and representing a third-order sequence (see below). According to Kókay (1996), the uppermost part of the Badenian was eroded due to an important regression (type 2 third-order sequence boundary) so the Sarmatian lies on an unconformity (at 723-m depth). The Sarmatian is made of sands, limestones, light-grey clays and lignites, reflecting more shallow marine and even continental fresh water–paludal conditions.

Some aspects make a precise calibration of the time involved in the studied succession difficult: (a) the absence of a detailed biostratigraphic zonation, (b) the variability in the absolute age assigned for the involved stages (see Báldi et al. (2002) for an illustrative

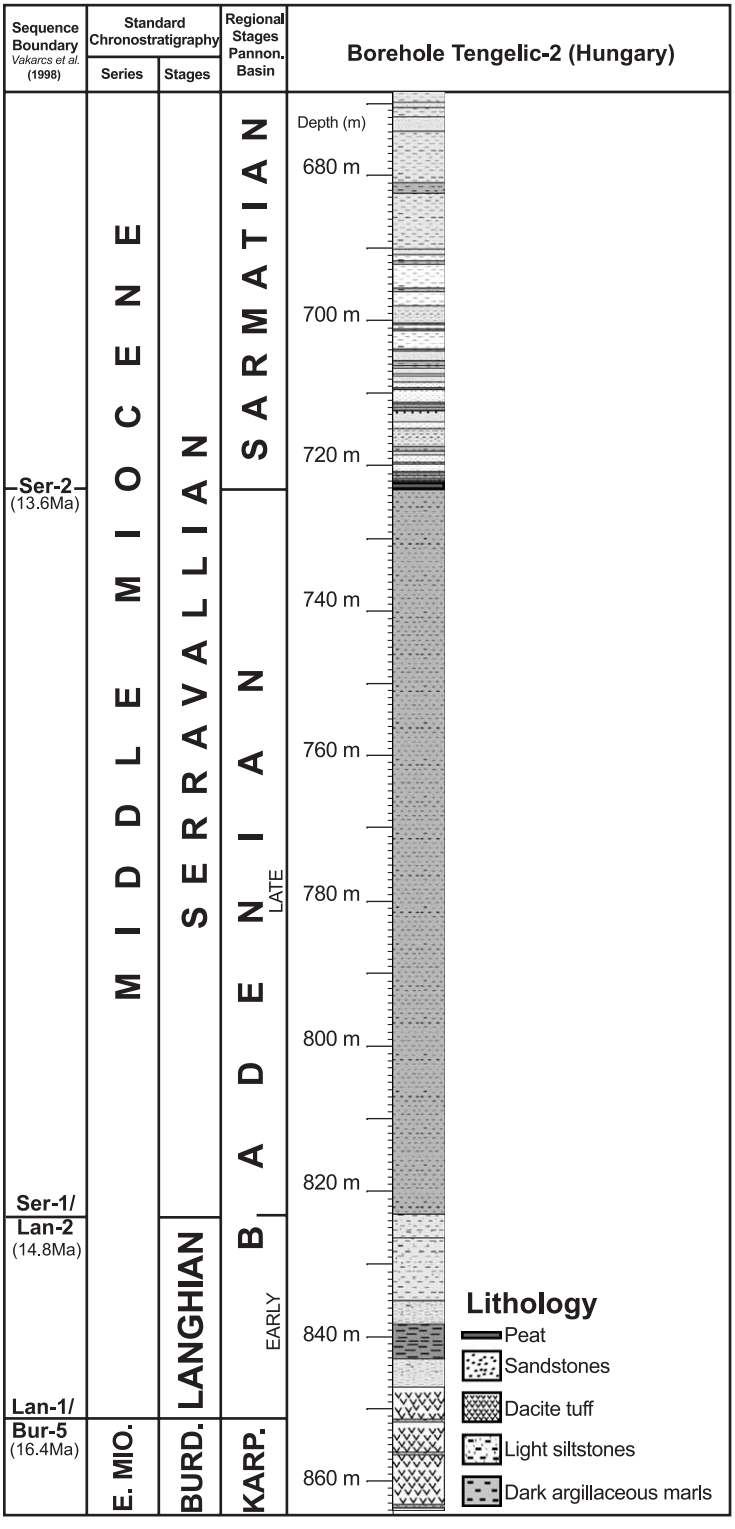
Sequence Boundary Vakarcs et al. (1998)
Standard Chronostratigraphy
Series
Stages
Regional Stages Pannon. Basin
Borehole Tengelic-2 (Hungary)
Depth (m)
680 m
700 m
720 m
740 m
760 m
780 m
800 m
820 m
840 m
860 m
Ser-2
(13.6Ma)
Ser-1/
Lan-2
(14.8Ma)
Lan-1/
Bur-5
(16.4Ma)
MIDDLE MIOCENE
E. MIO.
SERRAVALLIAN
LANGHIAN
BURD.
SARMATIAN
BADENIAN
LATE
EARLY
KARP.
Lithology
Peat
Sandstones
Dacite tuff
Light siltstones
Dark argillaceous marls

compilation) and (c) the possible existence of condensation and minor hiatuses (Báldi et al., 2002). Even so, an estimation could be determined. The selected part of the studied borehole, belonging to the middle Miocene, starts approximately at the Early/Late Badenian boundary. The substages of Vakarcs et al. (1998) for Middle and Late Badenian substages yield inconsistent ages, and they use Late Badenian. Thus, the Middle/Late Badenian boundary is considered coeval with the Langhian/Serravallian boundary. The Langhian/Serravallian boundary has usually been assigned to an absolute age of 14.8 Ma (i.e., Steininger et al., 1990; Berggren et al., 1995; Steininger et al., 1996, 1999; Vakarcs et al., 1998). The top of the selected part of the borehole for this comparison is difficult to precisely date but could be correlated with the sequence boundary Ser-2 differentiated by Vakarcs et al. (1998) and dated in as 13.6 Ma. Thus, the analysed succession could expand from 14.8 Ma to approximately 13.6 Ma, representing a time span of about 1.2 Ma. Assuming a constant rate of sedimentation for the 100.7-m-thick studied succession, a rate of sedimentation of 8.3 cm/ka is obtained. In the same studied area (SW Hungary), Báldi et al. (2002) calculated the rates of sedimentation from Tekeres-1 and Tengelic 2 boreholes during the Badenian period. In the Tekeres-1 borehole, a similar rate of sedimentation (13 cm/ka) is obtained, but for the Tengelic 2 borehole, the average sedimentation rate is much smaller (5 cm/ka). In the latter case, this could be a consequence of the relatively condensed Lower Badenian (interval not studied in our example), together with the existence of erosion in the uppermost part of the Badenian (Kókay, 1996; Báldi et al., 2002).

3.2. Sample collection and chemical processing

Pollen grains and dinoflagellate cysts are usually well preserved in the studied sediments. In this study, 78 samples of Karpatian, Badenian and Early Sarmatian ages have been analysed. However, during the Sarmatian, conditions were not very good for pollen preservation (e.g., sands and limestones), and some of the samples are sterile. Therefore, palynomorphs are generally scarce in materials of Sarmatian age (less than 700 grains/g of sediment) contrary to the Badenian sediments that contain more than 2000 grains/g and, in some cases, are very rich in dinoflagellate cysts (estimation of pollen concentration according to Cour (1974)). Spores have not been considered due to their near absence.

Sampling was made taking ca. 150 g of sediment per sample. In the chemical treatment, only a part (20–30 g of sediment) was used. The samples were treated with cold HCl (35%) and HF (70%), removing carbonates and silica. Separation of the palynomorphs from the rest of the residue was carried out using $ZnCl_2$ (density=2). Sieving was done through a 10-μm nylon sieve. The palynological residue, together with glycerine, was prepared on slides. A transmitting light microscope using ×250 and ×1000 (oil immersion) magnifications was used for pollen classification and counting. Pollen identifications were performed using the photograph bank of the laboratory in Lyon as well as the database "Photopal" (<http://www.mediasfrance.org/photopal>). After publication, the pollen data will be stored in the C.P.C. database (<http://www.mediasfrance.org/cpc>).

3.3. Taxonomical determination and differentiated groups

In this study, we used the botanical determination of pollen grains which is a novelty for the early–middle Miocene of the Pannonian basin. The botanical taxonomy of pollen grains allows us to know about the paleovegetation, ecology and climate (Suc and Bessedik, 1981). It has already been applied successfully for the Pliocene (Zagwijn, 1960; Pons, 1964; Suc, 1976; Drivaliari, 1993; Bertini, 1994; Popescu, 2001) and the Miocene (Naud and Suc, 1975; Bessedik, 1985; Zheng, 1990; Rivas-Carballo, 1991; Valle et al., 1995; Bertini et al., 1998; Barrón, 1999) knowing that all the living plant genera have been represented since the Eocene.

A minimum of 150 pollen grains, excluding *Pinus* and indeterminable (i.e., poorly preserved) Pinaceae and nondeterminate pollen grains, were counted in

Fig. 3. Geological log of the Karpatian–Sarmatian sediments of the borehole Tengelic 2 and chronostratigraphic framework. Biostratigraphy by Bohn-Havas (1982), Korecz-Laky (1982) and Nagymarosi (1982). Correlations and chronostratigraphic positions based on Berggren et al. (1995) and Steininger et al. (1990, 1996). Sequence stratigraphy by Vakarcs et al. (1998).

each analysed sample. Generally more than 30 different pollen taxa were found in each sample, and a total of 120 taxa have been identified in a total pollen sum varying between 247 and 3183 per sample.

Several studies (Turon, 1984; Hooghiemstra et al., 1986; Cambon et al., 1997) confirm that pollen grains found in modern sediments transported there by the air or river reflect the regional vegetation of the surrounding area, making paleoenvironmental and climatic interpretations dealing with fossil ones possible.

Based on the results of the pollen spectra, two different diagrams have been constructed:

(A) Simplified detailed pollen diagram (Fig. 4) without *Pinus* and indeterminable Pinaceae, where pollen percentages are calculated relative to the total pollen sum. Taxa with low percentages are grouped into the following groups: (1) megathermic (i.e., tropical) elements: *Acacia*, Euphorbiaceae, *Buxus bahamensis*, *Mussaenda* type, Rubiaceae, *Alchornea* type, *Fothergilla*, Melastomataceae, Rutaceae, Solanaceae, *Sindora*, *Eustigma*; (2) other swampy elements: indet. Taxodiaceae, *Myrica*, Cyrillaceae–Clethraceae, *Symplocos*, *Symplocos paniculata* type; (3) other mega-mesothermic (i.e., subtropical) elements: *Gingko*, Caesalpiniaceae, Theaceae, Myrtaceae, Agavaceae, Celastracae, *Rhoiptelea*, Araliaceae, Menispermaceae, *Corylopsis*, *Rhodoleia*, *Disanthus*, Loranthaceae, *Ricinus* type, *Cornus*; (4) other mesothermic (i.e., warm-temperate) elements: *Eucommia*, *Viburnum*, *Lonicera*, *Vitis*, *Parthenocissus*, *Rhus*, *Ostrya*, Rhamnaceae, Anacardiaceae, *Tamarix*, *Platanus*, *Hamamelis*, *Parrotia*, *Juglans* cf. *cathayensis*, *Fraxinus*, *Ligustrum*; (5) other herbs: Asteraceae Asteroideae type, Asteraceae Cichorioideae type, Campanulaceae, Brassicaceae, Thymelaceae, *Borrago*, *Sanguisorba*, *Galium*, Lamiaceae, Urticaceae, Caryophyllaceae, Plumbaginaceae, Malvaceae, Liliaceae, *Mercurialis*, *Artemisia*, *Ephedra*, Ranunculaceae, *Sparganium-Typha*, *Potamogeton*, Umbelliferae, Nymphaceae.

(B) Standard synthetic diagram without *Pinus* and indeterminable Pinaceae (Suc, 1984; Fig. 5), in which pollen taxa have been grouped into 10 different groups of taxa based on ecological criteria to clearly manifest temporal changes in vegetation: (1) megathermic elements: Euphorbiaceae, Rubiaceae, *Mussaenda*, Acanthaceae, *Alchornea*, *Fothergilla*, Melastomataceae, Rutaceae, Solanaceae, etc.; (2) mega-mesothermic elements: *Taxodium*, *Engelhardia*, *Platyacarya*, *Myrica*, *Sapotaceae*, *Distylium*, *Rhodoleia*, etc.; (3) *Cathaya*; (4) warm-temperate elements: *Quercus* deciduous type, *Carya*, *Acer*, *Juglans*, *Zelkova*, *Carpinus*, *Liquidambar*, etc.; (5) middle altitude trees: *Tsuga* and *Cedrus*; (6) high-altitude trees: *Abies* and *Picea*; (7) nonsignificant elements: Rosaceae, Ranunculaceae, non-identified pollen grains, etc.; (8) Cupressaceae; (9) Mediterranean xerophytes: *Quercus ilex-coccifera* type, *Olea* and *Phillyrea*; and (10) herbs and shrubs: Poaceae, *Plantago*, Amaranthaceae–Chenopodiaceae, Ericaceae, *Artemisia*, *Ephedra,* etc.

Dinoflagellate cysts have also been counted and classified. Their presence/absence and variations in concentration together with the pollen data give us information about paleobathymetry and paleoenvironment, a very useful tool in recognizing and characterizing eustatic changes.

3.4. Climatic reconstruction

Based on the pollen data, the climate has been estimated using the "climatic amplitude method" (Fauquette et al., 1998a,b). This method has already been applied to many pollen sequences of the western Mediterranean area (Fauquette et al., 1998a, 1999, in press; Fauquette and Bertini, 2003) and is applied here to the Tengelic pollen sequence described in the first part of the text. This will allow the climate in Hungary to be estimated for

Fig. 4. Pollen simplified detailed diagram of the borehole Tengelic 2 without *Pinus* and indeterminable Pinaceae. Taxa with low percentages are grouped into the following groups (see text for explanation).

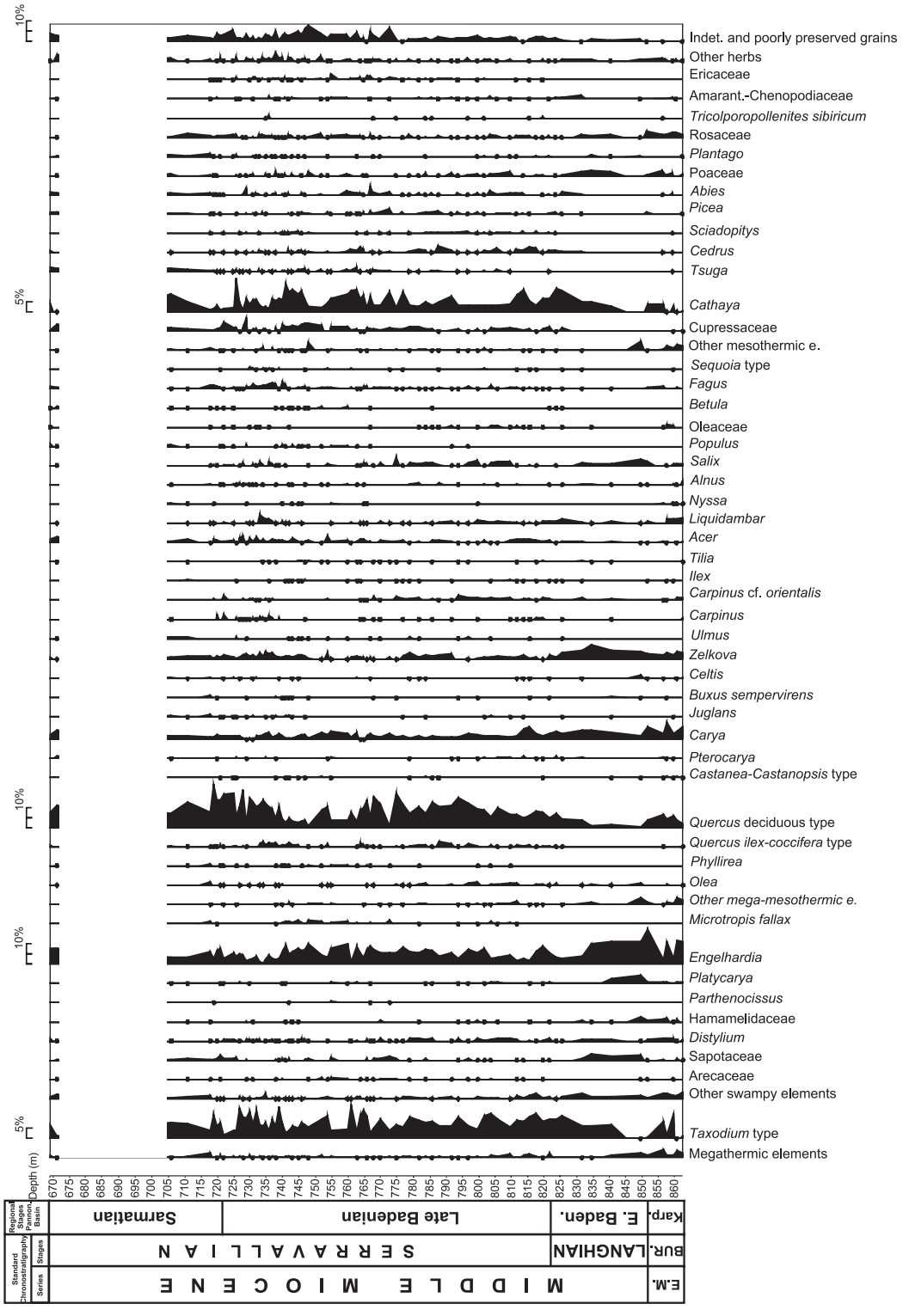
10%
5%
10%
10%
5%
Indet. and poorly preserved grains
Other herbs
Ericaceae
Amarant.-Chenopodiaceae
Tricolporopollenites sibiricum
Rosaceae
Plantago
Poaceae
Abies
Picea
Sciadopitys
Cedrus
Tsuga
Cathaya
Cupressaceae
Other mesothermic e.
Sequoia type
Fagus
Betula
Oleaceae
Populus
Salix
Alnus
Nyssa
Liquidambar
Acer
Tilia
Ilex
Carpinus cf. orientalis
Carpinus
Ulmus
Zelkova
Celtis
Buxus sempervirens
Juglans
Carya
Pterocarya
Castanea-Castanopsis type
Quercus deciduous type
Quercus ilex-coccifera type
Phyllirea
Olea
Other mega-mesothermic e.
Microtropis fallax
Engelhardia
Platycarya
Parthenocissus
Hamamelidaceae
Distylium
Sapotaceae
Arecaceae
Other swampy elements
Taxodium type
Megathermic elements
Depth (m)
670 675 680 685 690 695 700 705 710 715 720 725 730 735 740 745 750 755 760 765 770 775 780 785 790 795 800 805 810 815 820 825 830 835 840 845 850 855 860
Standard Chronostratigraphy
Series
Stages
Regional Stages Pannon Basin
MIDDLE MIOCENE
SERRAVALLIAN
LANGHIAN
Sarmatian
Late Badenian
E. Baden.
E.M.
BUR.
Karp.

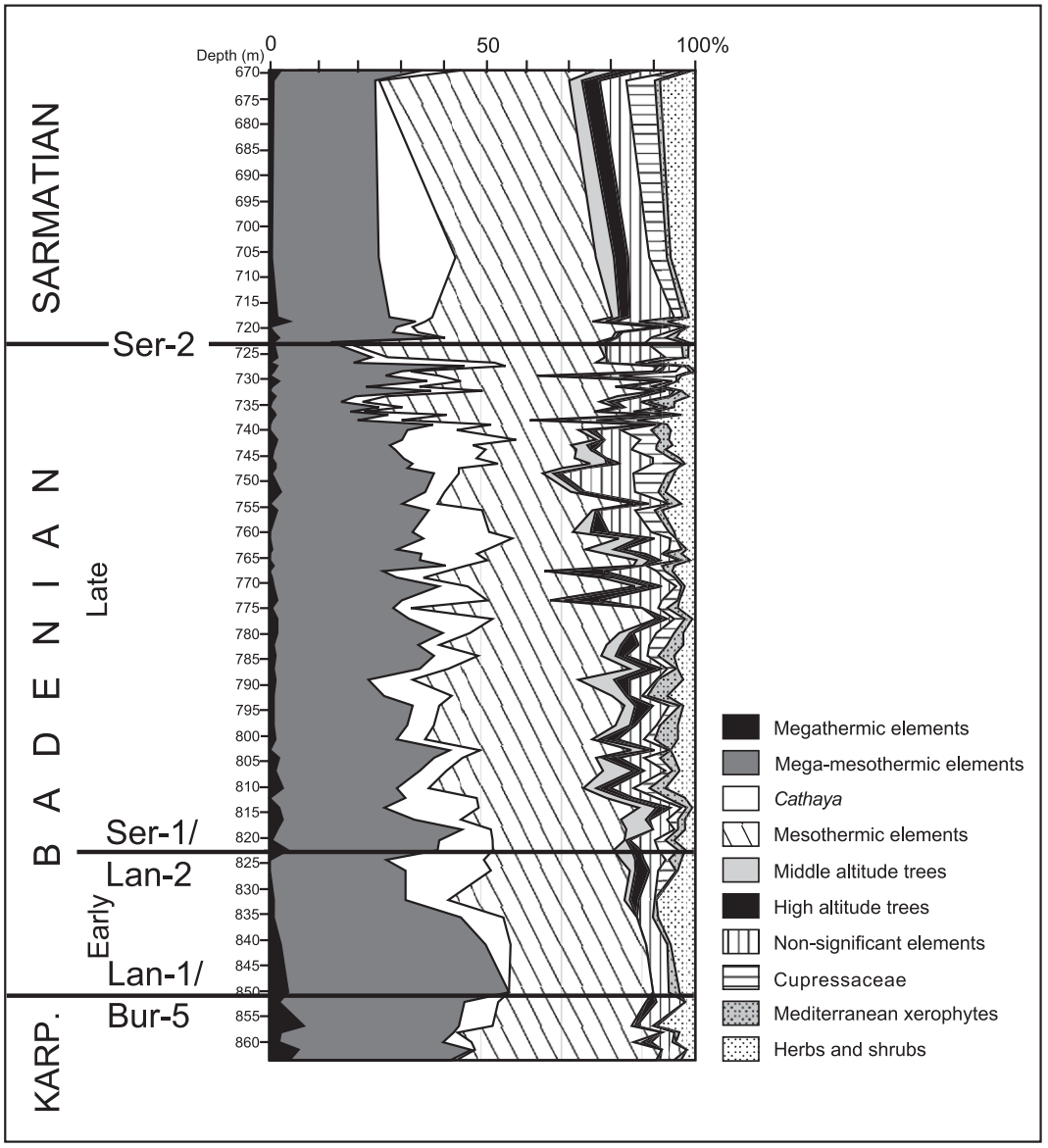

Fig. 5. Pollen synthetic diagram without *Pinus* and indeterminable Pinaceae of the Tengelic 2 borehole. Grouping was made regarding the ecology of the plants (see text for explanation).

the middle Miocene period. The past climate is estimated by transposing the climatic requirements of the maximum number of modern taxa to the fossil data. The low-latitude/altitude taxa were separated from the high-latitude/altitude taxa and used in the reconstruction process. The estimates obtained therefore correspond to the climate at low to middle–low altitude, as described in Fauquette et al. (1998a). The pollen grains of *Pinus* and indeterminable Pinaceae have been excluded from the pollen sum (Fauquette et al., 1998a, 1999). The pollen grains of these taxa are over-represented in the marine (coastal) sediments due to its prolific production and overabundance in air and water transport (Heusser, 1988; Suc and Drivaliari, 1991; Cambon et al., 1997; Beaudouin, 2003).

3.5. Cyclostratigraphic analysis

Although pollen data are efficient paleoclimate indicators, the use of palynological data in cyclostratigraphic research is comparatively scarce. Some articles demonstrate the usefulness of pollen analysis as evidence for Milankovitch induced climatic fluctuations through comparison between lithological data, pollen diagrams and Milankovitch curves (i.e., Okuda et al., 2002; Nádor et al., 2003). However, only occasionally is spectrum analysis applied to time series obtained from pollen records (i.e., Mommersteeg et al., 1995; Popescu, 2001; Popescu et al., in press).

A part of the studied succession (the stratigraphic interval between 826.4 and 725.7 m) was chosen for cyclostratigraphic analysis. This part of the succession is characterized by a similar lithology and the absence of sedimentary breaks (condensed intervals, erosional surfaces, etc.) that could alter a possible cyclicity. Thus, we can assume a constant sedimentation rate along the analysed section.

The cyclostratigraphic analysis was performed on a time series of pollen data on the relative abundance of the two differentiated groups, thermophilous and altitudinal trees, throughout the studied interval. Even if the sampling procedure was not carried out with a cyclostratigraphic perspective, most of the sample sites throughout the interval are at a constant sampling rate (around 1–2 m). The total thickness of the analysed section is 100.7 m.

Cyclostratigraphic analysis was performed on a sequence of 101 data obtained with a constant sampling of 1 m. The first step was the subtraction of the experimental mean of the sequence to evaluate any possible trend. No distinctive trend was observed, and then the zero-mean series was used as an input to differentiate the spectral estimator. To approach the cyclostratigraphic analysis, several power spectrum estimators were applied. As often occurs in statistics, there is no estimator consistently superior to the others, particularly when using real data (case study vs. simulated data). However, for example, some estimators may be more efficient in dealing with short sequences, but a difficult problem then is how to define a short sequence. Hence, a general strategy recommended for spectral analysis in cyclostratigraphy is to report the results obtained using several methodologies from those most frequently used in cyclostratigraphy (Schwarzacher, 1975, 1993; Pardo-Igú et al., 1994, 2000).The spectral estimators selected were (a) Blackman–Tukey approach, (b) maximum entropy estimator and (c) Thomson multitaper approach. The Blackman–Tukey approach was applied using 25 values of the correlation lags (M) and with the lag window of Tukey. Then $M \approx N/4$, N being the number of measurements (N=101). This method presents the smoothest spectrum, showing broad but significant peaks. To evaluate the significance of the registered peaks, a background of red noise spectrum has been added, together with 90%, 95% and 99% confidence intervals. The same value of correlation lags (M=25) was used with the maximum entropy estimator. Maximum entropy maintains practically the same location for the peaks but, in this case, their definition. Finally, five tapers were used with the Thomson multitaper method, and the series was padded with zeros up to four times its original length, as recommended by Thomson (1982). In general, the Thomson multitaper shows the spectra characterized by a higher number of peaks, which are especially well defined. This approach is useful in locating the frequency of spectral peaks although many of them are spurious. According to the above information, frequency identification (2) of the spectral peaks will be obtained in the most conservative and then objective way; that is, when the spectral peak was not well defined, we prefer to refer it to the frequency band in which it is included.

4. Results

4.1. Pollen analysis and climatic parameters

Apart from the dominance of *Pinus* and indeterminable Pinaceae, pollen spectra show that mega-mesothermic (*Taxodium*, *Engelhardia*, Sapotaceae and *Myrica* mainly) and mesothermic (such as *Quercus* deciduous type and *Carya*, etc.) elements were the most abundant. *Cathaya*, a gymnosperm living today in the subtropical mid-altitude forest of southern China, is also extensively represented. Mid-altitude and high-altitude elements, such as *Cedrus*, *Tsuga*, *Abies* and *Picea*, appear in a great number. Small amounts of megathermic elements, such as Euphorbiaceae, Rubiaceae, *Mussaenda* type, *Alchornea* type, Melastomata-

ceae, *Acacia*, *Sindora* or Rutaceae, occur in all the samples (Figs. 4 and 5). Percentages of the rest of the groups are not very high.

Reconstructed climatic parameters from the "climatic amplitude method" (Fauquette et al., 1998a,b; Fig. 6) allow for the characterization of values of mean annual temperatures (Ta) mainly between 18 and 20 °C. The mean temperatures of the coldest month (Tc), which play an important role in controlling the vegetation (Quézel and Médail, 2003), vary from 12 to 15 °C. Estimated values of mean annual precipitation (Pa) are generally between 1200 and 1400 mm.

4.2. Pollen distribution and stratigraphic changes

Changes in pollen flora of different order along the borehole have been observed (Figs. 4 and 5).

(1) The major change is the observed impoverishment in plant diversity produced by the disappearance of thermophilous plants (*Acacia*, *Buxus*

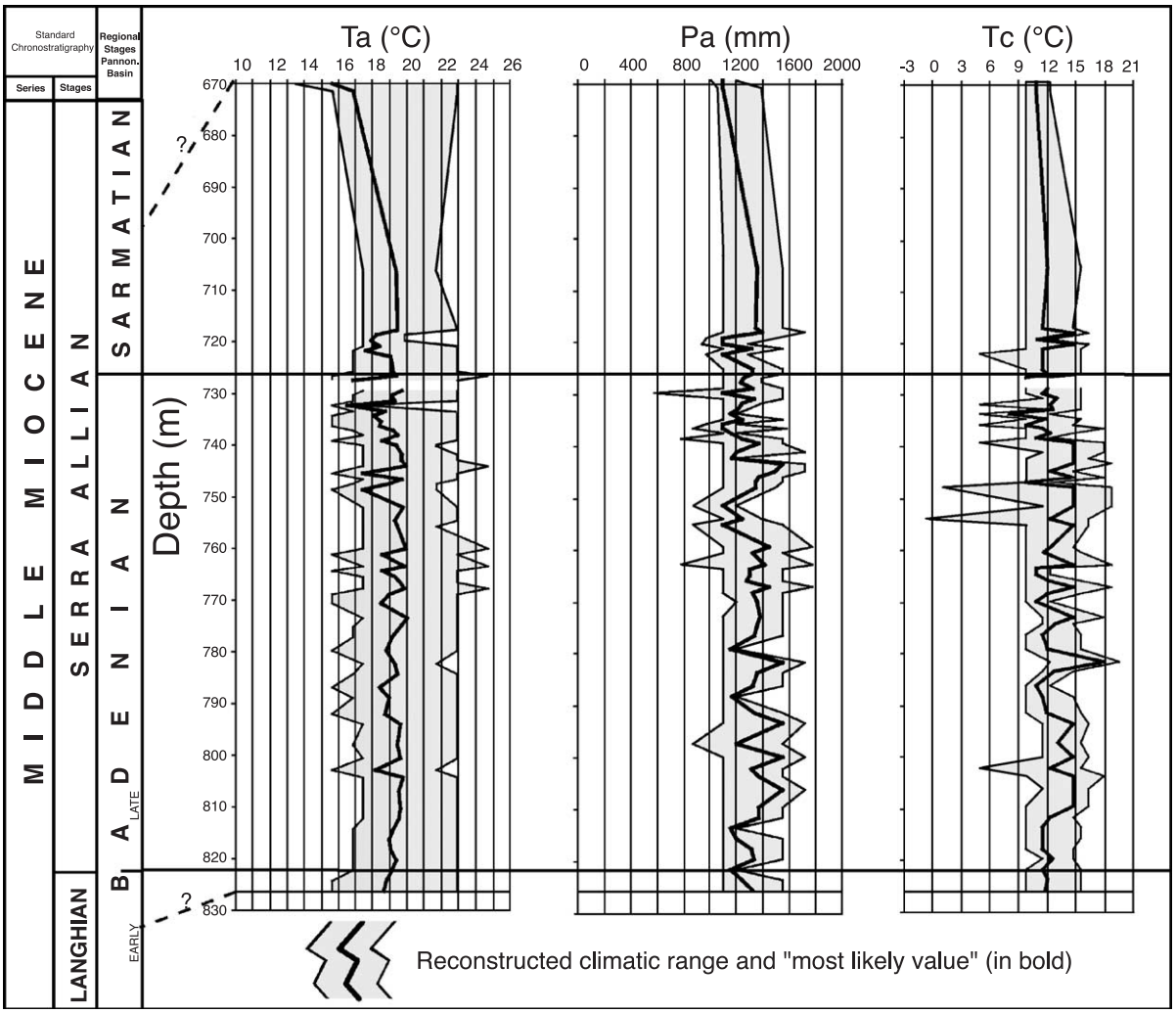

Fig. 6. Reconstructed climatic values of mean annual temperature (Ta in °C), mean annual precipitation (Pa in mm) and mean temperature of the coldest month (Tc in °C) of the late Early Badenian to Sarmatian stages of the borehole Tengelic 2.

bahamensis type, Chloranthaceae, Acanthaceae, etc.) and the consequent enrichment in mesothermic plants (mainly *Quercus* deciduous type, Alnus, etc.) from the Badenian to the Sarmatian. This change has also been observed and estimated using the "climatic amplitude method" (Fauquette et al., 1998a,b). A progressive decrease in the mean annual temperatures from about 20 °C in the Badenian to 16 °C in the Sarmatian and the mean annual precipitation from around 1550 to ca. 1100 mm are observed (Fig. 6).

(2) Secondary changes in the vegetation have been noticed along the borehole. There were alternations of periods in which thermophilous plants (mainly mega-mesothermic and swampy plants) were well developed and others where altitudinal elements are more abundant. Close to the Badenian/Sarmatian boundary, these alternations became more exaggerated (see Fig. 5). This fact was also observed by Andreanszky (1959) after studying the macrofloras close by.

4.3. Spectral analysis of pollen data

Before the analysis of the registered spectral peaks, it is necessary to consider the frequency range that probably has more possibilities of being registered. On one hand, according to the sampling interval (usually between 1 and 2 m), those peaks corresponding to thickness lower than 2 m (i.e., those in the range of the highest frequencies) have less possibilities of being registered. On the other hand, those cycles on the edge of the low frequencies close to the vertical axis must be considered carefully; thus, those peaks at frequencies lower than 0.0293 (corresponding to around 34.13 m) were not considered. Thus, the frequency range of interest was between 0.0293 and 0.495, corresponding to cycles with a thickness between 34.13 and 2.02 m.

4.3.1. Thermophilous component

Several peaks have been registered at similar frequency values (cycles per sampling interval) and the corresponding wavelengths (thickness; Fig. 7, Table 1).

In the Blackman–Tukey approach, four bands are registered at the lower, middle and higher frequencies. In the range of the lower frequencies, a wide band with two more prominent peaks is registered, corresponding to frequencies of 0.0495 (20.20 m) and 0.129 (7.77 m), the later being significant above the 95% of Cl. At middle frequencies, a wide band is registered around the 90% of Cl, between 0.198 (5.05 m) and 0.248 (4.04 m). Two smoothed peaks appear above the background around 0.356 (2.81 m) and 0.436–0.446 (2.30–2.24 m).

In the maximum entropy spectrum, peaks are at similar frequencies to those in the Blackman–Tukey approach. In the lower frequencies, the two peaks are separated at 0.0495 (20.20 m) and 0.119–0.129 (8.42–7.77 m). At the middle frequencies, two well-defined peaks are registered at 0.198 (5.05 m) and 0.248 (4.04 m). Less significant and defined are the peaks in the highest frequencies at 0.347 (2.89 m) and 0.426–0.436 (2.35–2.30 m).

In the Thomson Multitaper analysis, the numerous peaks are mainly located in some frequency band. In the lower frequency, several significant peaks are registered at 0.0293–0.0391 (34.13–25.6 m) and 0.0547–0.0762 (18.29–13.13 m). A conspicuous peak is present at 0.102 (9.85 m). In higher frequencies, differentiation becomes more difficult, but three groups of minor peaks are registered at 0.197–0.248 (5.07–4.04 m), 0.342–0.371 (2.93–2.69 m) and 0.422–0.449 (2.37–2.23 m).

The comparative analysis between the three methods allows for a differentiation of five frequency bands in which peaks of different significance have been registered (Table 2): (a) 0.0293–0.0547 (34.13–18.29 m) and 0.0495–0.0762 (20.20–13.13 m), with special relevance for the interval at 0.0293–0.0495 (34.13–20.20 m); (b) 0.102–0.129 (9.85–7.77 m); (c) 0.198–0.248 (5.05–4.04 m), being a wide band or two significant peaks; (d) 0.342–0.371 (2.93–2.69 m), especially at 0.347–0.356 (2.89–2.81 m) and (e) 0.422–0.449 (2.37–2.23 m). From these, the most significant peaks are in the lower frequencies while those corresponding to the higher ones are comparatively less evident.

4.3.2. Altitudinal trees

In the Blackman–Tukey approach (Fig. 7, Table 1), two peaks are well differentiated, above 95% Cl, at 0.0495–0.0594 (20.20–16.83 m) and 0.198–0.208 (5.05–4.81 m) (90% Cl), and there is also a wide smoothed band at 0.347–0.386 (2.89–2.59 m; 90%

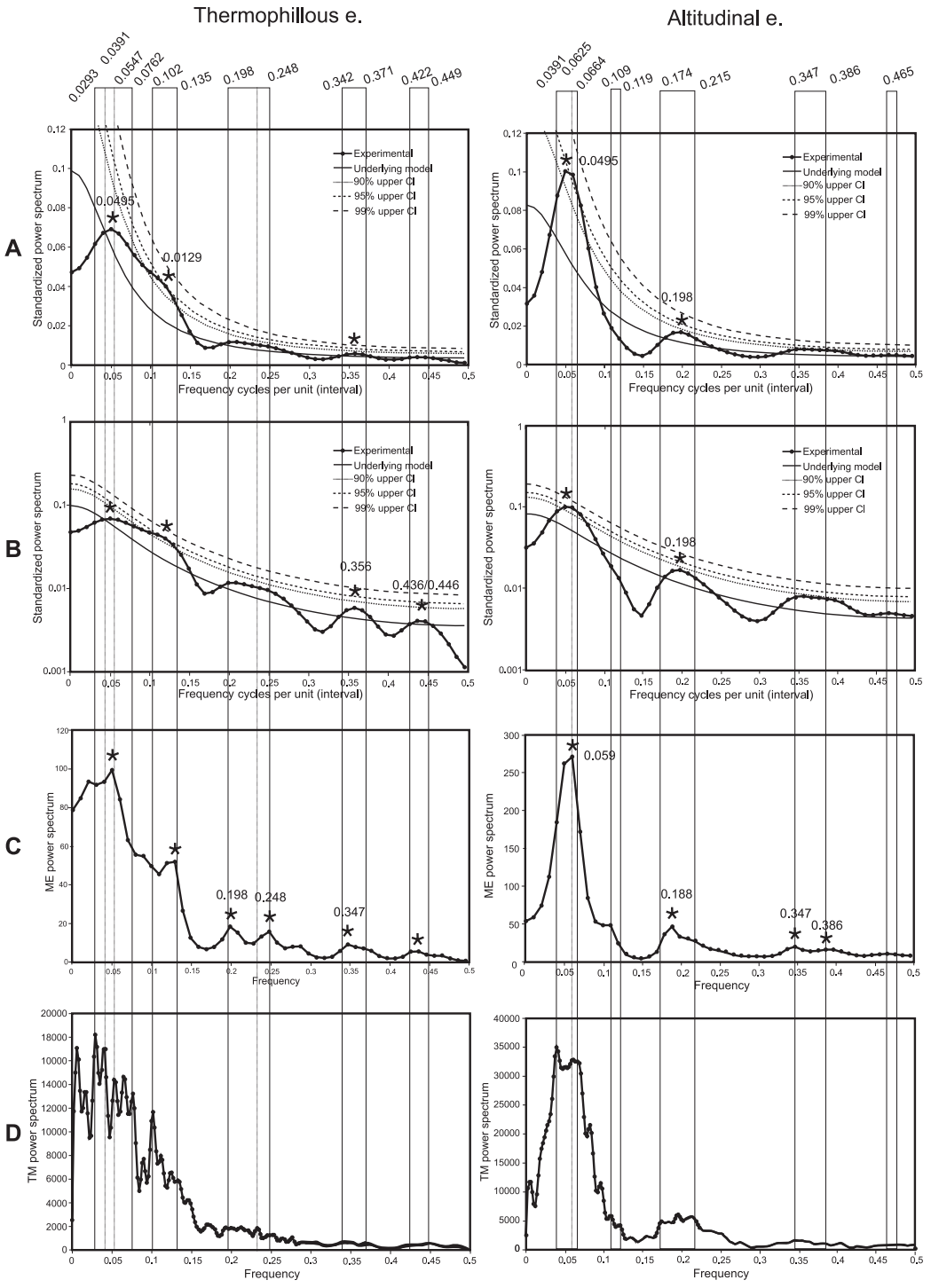

Fig. 7. Pollen data spectral analysis of the borehole Tengelic 2 for the two differentiated elements: thermophilous and altitudinal trees. (A, B) Blackman–Tukey with Tukey window and M=25. (C) Maximum entropy estimator with M=25. (D) Thomson multitaper approach. Stars over the most significant peaks show the registered frequency values.

Table 1
Frequency and thickness (m) of peaks registered in the spectral analyses (BT—Blackman–Tukey; ME—maximum entropy; TM—Thomson multitaper) of the two selected elements (Ther.—thermophilous; Alti.—altitudinal trees)

		Ther. BT	Ther. ME	Ther. TM	Alti. BT	Alti. ME	Alti. TM
Frequency	Thickness						
0.0293	34.13			X			
0.0391	25.6	x		X			X
0.0396	25.2	x	x				
0.0495	20.20	X	X		X	x	
0.0547	18.29	x		X			
0.0594	16.83				x	X	X
0.0605	16.52						X
0.0664	15.06			X			
0.0762	13.13			X			
0.1016	9.85			X			
0.1188	8.42		x				
0.1288	7.77	X	X				
0.1777	5.63						X
0.1881	5.32				x	X	
0.1973	5.07			X			X
0.1980	5.05	x	X	X	X		
0.2079	4.81	x		X	x		
0.2148	4.65	x		X			X
0.2475	4.04	x	X	X			
0.3418	2.93			X			
0.3465	2.89	x	X	X	x	X	
0.3564	2.81	X	x	X	x		
0.3663	2.73	x					
0.3711	2.69	x		X	x		
0.3762	2.66				x		
0.3861	2.59				x	X	
0.4219	2.37			X			
0.4258	2.35		x	X			
0.4355	2.30	x	x	X			
0.4455	2.24	x		X			
0.4492	2.23			X			
0.4648	2.15				x		
0.4752	2.10				x		

Cross size related to relevance of the registered peak.

Cl). A much smoother peak is registered at 0.465–0.475 (2.15–2.10 m).

In the maximum entropy spectrum, peaks are better differentiated at 0.0495–0.0594 (20.20–16.83 m) and 0.188 (5.32 m). In the higher frequencies, two smaller peaks are registered at 0.347 (2.89 m) and 0.386 (2.59 m).

In the Thomson Multitaper analysis at the lower frequency, several significant peaks are registered at 0.0391–0.0605 (25.6–16.52 m). At intermediate frequencies, a band is characterized at 0.178–0.197–0.215 (5.63–5.07–4.65 m), while at higher frequencies, there is not a clear differentiation.

The comparative analyses allow for a differentiation of the following (Table 2): (a) relevant peaks at 0.0391–0.0594 (25.6–16.83 m); (b) a smoothed peak at 0.178–0.197–0.215 (5.63–5.07–4.65 m), especially at 0.188–0.198 (5.32–5.05 m) and (c) a wide band or two separated peaks at 0.347–0.386 (2.89–2.59 m).

4.3.3. Thermophilous vs. altitudinal trees

A preliminary comparison allows us to recognize a different pattern in the spectral analysis, with some peaks at similar frequencies. Thus, while peaks belonging to the lower frequencies are better differentiated in the altitudinal group, those from the higher frequencies are comparatively better expressed in the thermophilous group.

The two groups show some peaks registered at similar bands; (a) in the lower frequencies, a relatively wide band is registered at 0.0293–0.0495 (34.13–20.20 m) in thermophilous and 0.0391–0.0594 (25.6–16.83 m) in altitudinal; (b) at intermediate frequencies, a wide band or two peaks are registered at 0.198–0.248 (5.05–4.04 m) in thermophilous or a peak at 0.174–0.215 (5.63–4.65 m) in altitudinal, with a peak of especial significance at 0.188–0.198 (5.32–5.05 m) in both groups; and (c) a smoothed peak at 0.342–0.356 (2.93–2.89 m) in thermophilous or a wide band/two peaks at 0.347–0.386 (2.89–2.59 m) in altitudinal.

Table 2
Frequency and thickness (m) of the selected peaks (according significance) registered in the spectral analyses of the two analyzed groups

		Ther. BT	Ther. ME	Ther. TM	Alti. BT	Alti. ME	Alti. TM
Frequency	Thickness						
0.0293	34.13			X			
0.0495	20.20	X	X		X	x	
0.0594	16.83				x	X	X
0.1016	9.85			X			
0.1288	7.77	x	X				
0.1881	5.32				x	X	
0.1980	5.05	x	X	X	X		
0.3465	2.89	x	X	X	x	X	
0.3861	2.59				x	X	
0.4219	2.37			X			
0.4492	2.23			X			

Legend as in Table 1.

Other peaks are not registered in the two groups but are mainly found in one of them. Thus, at the highest frequencies, peaks are mainly registered in thermophilous at frequencies of 0.422–0.449 (2.37–2.23 m). Peaks at frequencies around 0.102–0.129 (9.85–7.77 m) are less relevant and mainly registered in thermophilous.

4.4. Dinoflagellate cyst distribution

Dinoflagellate cysts are abundant in the samples. Characteristic dinocysts of open marine conditions, such as *Nematosphaeropsis labyrinthus*, *Spiniferites* sp., *Labyrinthodinium trumcatum*, *Cerebrocysta piaseckii*, *Cordosphaeridiridum minimum*, *Tectatodinium pellitum* and *Unipontidinium aquaeductum*, have been found (Wall et al., 1977; Harland, 1983; Turon, 1984). However, they are not found at the Karpatian/Badenian boundary (851.3 m depth; Fig. 8). During the Early Badenian and later on during the Late Badenian, the percentage of dinocysts in the samples is high. Nevertheless, their percentage decreases gradually during the last part of the Late Badenian. Together with the rest of dinoflagellate cysts, totally disappeared at the Badenian/Sarmatian boundary (Fig. 8). Later, the diversity was reduced to the point that only a few cosmopolitan low saline tolerant species persisted in the Sarmatian (*Lingulodinium machaerophorum, Spiniferites* spp., *Operculodinium centrocarpum-israelianum*, *Polysphaeridium zoharyi*, *Polysphaeridium* sp. and *Cleistosphaeridium placacanthum*).

5. Interpretation and discussion

5.1. Vegetation and climatic conditions

The vegetation, according to the high percentage of trees in the pollen spectra, is typical of a forest. As a large number of taxa have been identified and classified in this study, they can also be compared to the organization in altitudinal belts of the present-day vegetation in southeastern China (Wang, 1961; Axelrod et al., 1996), the closest living example of this floral inventory (Suc, 1984).

Therefore, the vegetation could be grouped into ecologically different environments:

(1) seacoastal environment represented by saline-bearing elements, such as Amaranthaceae–Chenopodiaceae, *Ephedra,* Plumbaginaceae and *Tamarix*;
(2) swamp environment characterized by *Taxodium* type as the most important component, *Myrica*, *Nyssa* cf. *sinensis*, Sapotaceae, Cyrillaceae–Clethraceae and *Symplocos*;
(3) deciduous–evergreen mixed forest which developed at a higher altitude composed mainly of *Quercus* deciduous type, *Engelhardia*, *Platycarya*, *Carya*, *Fagus*, *Distylium*, Hamamelidaceae, *Carpinus*, *Celtis*, *Zelkova* and *Acer*; within this vegetation belt, a riparian plant association has been identified with *Salix* and *Alnus*; the shrub level was dominated by Ericaceae, *Ilex*, Caprifoliaceae, Rhamnaceae, Rosaceae, etc;
(4) mid-altitude forest characterized by the abundance of pollen grains of gymnoperms, such as *Pinus*, *Cathaya*, *Sciadopitys*, and a smaller amount of *Cedrus* and *Tsuga*; and
(5) high-altitude forest depicted by low percentages of *Abies* and *Picea*.

After interpreting the pollen flora, a subtropical to warm-temperate humid climate has been inferred. Climate was also quite humid to support the development of such a large association of thermic elements (of present-day "Asiatic" affiliation and climate) which requires very humid conditions all year (Wang, 1961). These floral assemblages during the Karpatian and Early Badenian of the borehole Tengelic 2 clearly reflect the Miocene Climatic Optimum (MCO). These floras are very rich in mega-mesothermic elements (thermophilous elements), such as *Acacia*, Chloranthaceae, *Buxus bahamensis-mexicana* type, Caesalpiniaceae, *Mussaenda* type, Rubiaceae, Euphorbiaceae, Sapotaceae, *Engelhardia*, *Platycarya*, Cyrillaceae–Clethraceae, etc. (Fig. 9).

The obtained values for mean annual temperatures (Ta) and mean annual precipitation (Pa) are higher compared to those estimated by Ivanov et al. (2002) for the Badenian and Sarmatian of a relatively close area, the Forecarpathian Basin in Bulgaria (Ta=16–18 °C, Pa=1100–1300 mm during the Badenian and Ta=13.3–17 °C and Pa=650–750 mm during the Sarmatian). Similar climatic interpretations (subtropical to warm temperate climate)

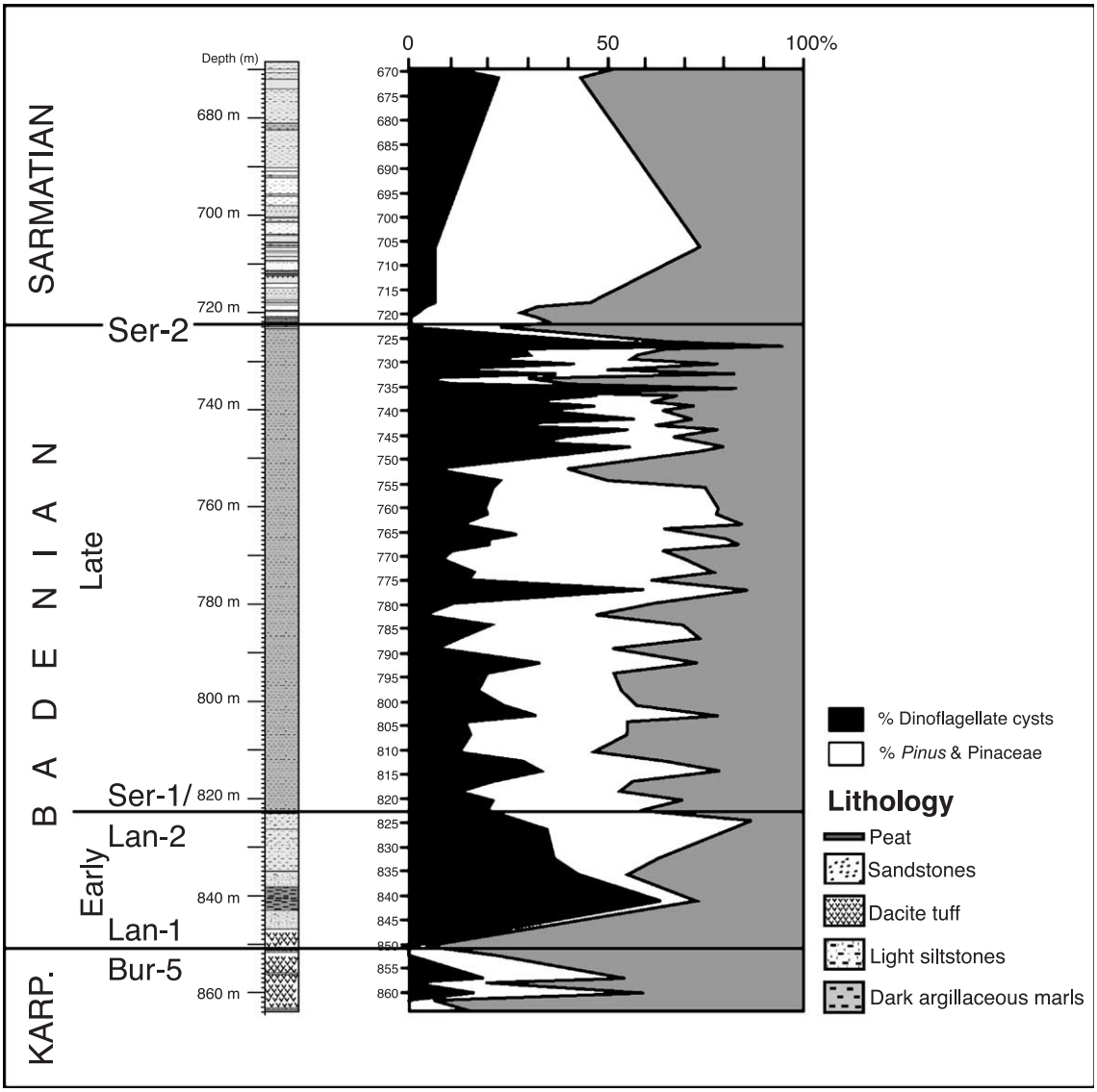

Fig. 8. Comparison between the concentration of *Pinus* and indeterminable Pinaceae and dinoflagellate cysts in the pollen record of the Tengelic 2 borehole. Sequence boundaries Bur-5/Lan-1 and Ser-2 are very well evidenced in the palynological analysis by the absence of dinocysts and an important decrease in the percentage of *Pinus* and indeterminable Pinaceae. Climatic cooling as a consequence of the development of the EAIS (East Antarctic Ice Sheet) is the cause of such a regression in the Ser-2 sequence boundary (Late Badenian–Sarmatian boundary).

were made after the study of nannofloras (Nagymarosi, 1982) and molluscs (Bohn-Havas, 1982) of the borehole. These estimated high-temperature values are in accordance with the observed presence of coral reefs in the Hungarian area during the Badenian (Saint Martin et al., 2000).

5.2. Climatic variations during the late early–middle Miocene

5.2.1. Monterey cooling event

The major change registered in plant diversity and climatic parameters is related to a gradual decrease in

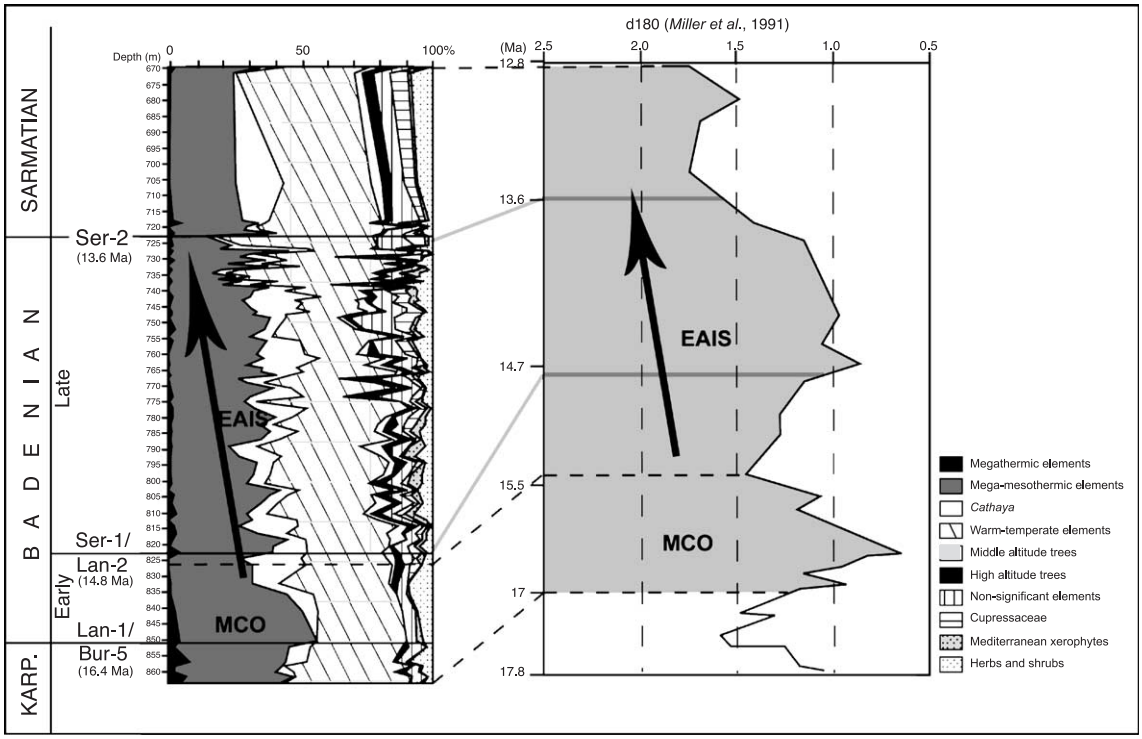

Fig. 9. Comparison between the pollen synthetic diagram of the borehole Tengelic 2 and the isotopic curve of Miller et al. (1991). The highest percentages of megathermic and mega-mesothermic elements are registered during the Karpatian and Early Badenian as a floral response to the MCO (Miocene climatic optimum). During the Late Badenian and Sarmatian stages, floral assemblages are progressively poorer in these elements and consequently richer in temperate elements. The diversity also decreases. This has been interpreted as a vegetal reaction to the increase in the development of the East Antarctic Ice Sheet (EAIS), thus a global cooling.

temperatures and precipitation right after the MCO. Similar but lower results are described and estimated by Ivanov et al. (2002) in the Forecarpathian Basin (central Paratethys area, northwest Bulgaria) for the Badenian–Sarmatian ages.

This fact is well documented worldwide and has been correlated with the general decrease in temperature observed by several authors as a gradual increase in the isotopic $\delta^{18}O$ values took place (DSDP sites 608 in Miller et al. (1991) and 588 in Zachos et al. (2001a) during this timespan called "Monterey Cooling Event" and related to the increase in the development of the East Antarctic Ice Sheet (EAIS; Flower and Kennett, 1994; Fig. 9).

5.2.2. Long-term Milankovitch-scale variations

The alternations of predominance in thermophilous plants (warm period), with intervals where altitudinal elements (cool period) are more abundant, could be related to cyclic climatic changes. Climatic changes made the vegetation belts "move" up during a warmer period and down when there were cooler conditions. In cooler conditions, the swamp environment is further reduced and occupied mostly by the deciduous–evergreen mixed forest, and the influence of plants from mid- and high-altitude forest is higher (Fig. 10A). In warmer and humid periods, the swamp gains land in comparison to the other higher belts displacing them upwards; this means a higher percentage in subtropical and swampy elements and a lower one in deciduous–evergreen mixed forest and in mid-high altitude forest (Fig. 10B).

The comparison of our pollen results with isotopic data and eccentricity–insolation curves is significant in interpreting the cause of such cyclical changes. Even considering the difficulties for a calibration of the absolute time involved in the studied interval, the tuning of these vegetation changes to the eccentricity

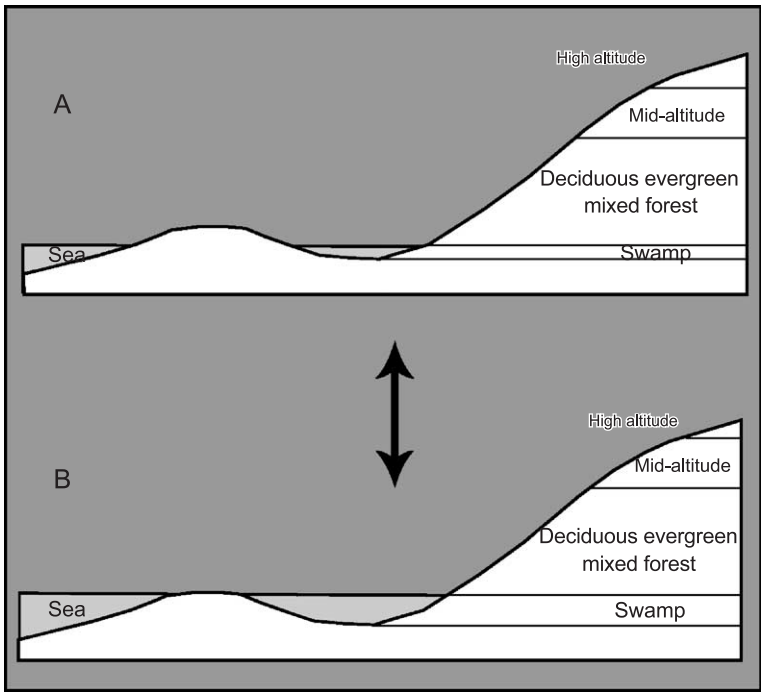

Fig. 10. Sketch of the organization of the vegetation in altitudinal belts during the Badenian–Sarmatian in the Pannonian basin. (A) Cold and dry period: high presence of deciduous–evergreen mixed forest and middle- and high-altitude elements. (B) Warm–humid period with a good development of the swamp and less influence of the deciduous–evergreen mixed forest and mid–high-altitude forest.

and insolation time series of the $La93_{(1,1)}$ solution and to the isotopic curve of Zachos et al. (2001a) is rather consistent and some discrepancies may be due to small changes in sedimentation rates (Fig. 11).

5.2.3. Long- to short-term Milankovitch-scale variations

The obtained spectral analysis were interpreted following the two most common ways: (1) analysing the ratios between their corresponding frequencies and (2) characterizing their time duration.

(1) The most conservative option is to characterize the ratio between the frequencies of the peaks registered and compare them to those proposed for the usual cycles registered in the stratigraphic record, the Milankovitch cycles. As concluded before, the spectral peaks differentiated in the two groups are 0.0293–0.0495–0.0594 (34.13–20.20–16.83 m), 0.102–0.129 (9.85–7.77 m), 0.188–0.198 (5.32–5.05 m), 0.347–0.386 (2.89–2.59 m) and 0.422–0.449 (2.37–2.23 m). For the Miocene, the values of the main astronomical periods can be considered similar to those at present, for precession (P1–P2, 19,000–23,000 years), obliquity (O1–O2, 41,000–54,000 years) and eccentricity (E1–E2–E3, 95,000–123,000 years for short term and 413,000 years for long term; Berger et al., 1989, 1992). As usual, if we consider as 1 the P1=19,000, the estimated ratios between the frequencies of the Milankovitch cycles will be around 1:1.21:2.16:2.84:5.00:6.47:21.74 (Table 3). Estimated ratios for other usual cycles interpreted as the combined effect of precession and obliquity (O+P; Berger, 1977) at periodicities of 59,000–64,000 will be 3.11:3.37 (Table 3). To analyse the ratios between the registered peaks, two options could be proposed (Table 4):

– Option A: If we consider the highest frequency, those at 0.449 (2.23 m) as 1, the ratio between the frequencies registered in our spectral analysis will be 1:1.06:1.16:1.29:2.26:2.39:3.48:4.40:7.56:9.07:15.3. The

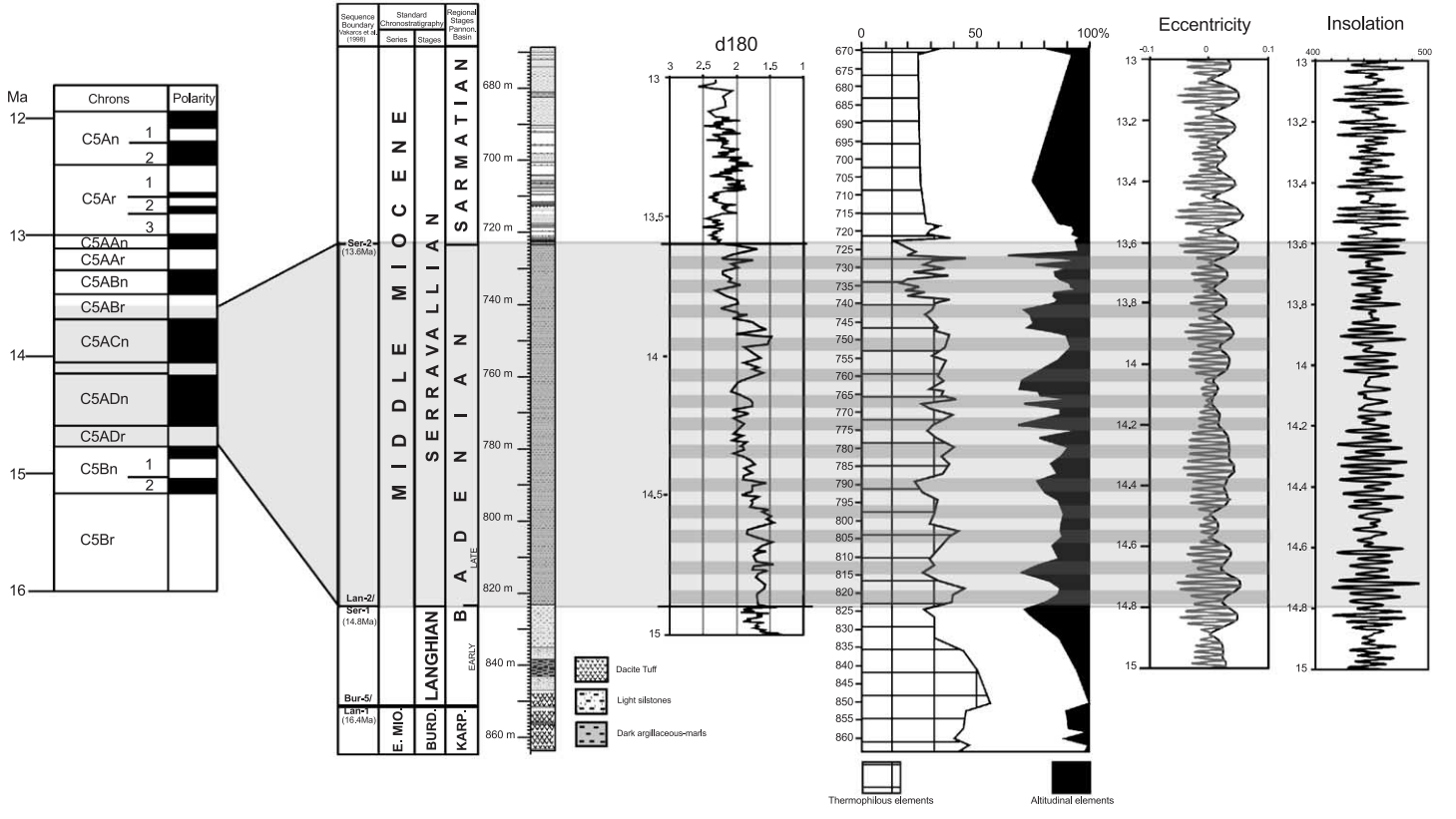

Fig. 11. Comparison between the thermophilous elements–Altitude trees of the Tengelic-2 borehole compared with the $\delta^{18}O$ curve for the middle Miocene (Zachos et al., 2001a) and the eccentricity and insolation curves of Laskar's solution $La90_{(1,1)}$ (Laskar, 1990; Laskar et al., 1993) for the studied time span (Late Badenian) from 13.6 to 14.8 Ma (Vakarcs et al., 1998). Miocene time scale is after Berggren et al. (1995). Shaded areas show concordances between these parameters for the borehole Tengelic 2 (Late Badenian age).

Table 3
Ratios of the main Milankovitch cycles during the Miocene

Period	Ratios
E_3=413,000	21.74
E_2=123,000	6.47
E_1=95,000	5.00
O+P=64,000	3.37
O+P=59,000	3.11
O_2=54,000	2.84
O_1=41,000	2.16
P_2=23,000	1.21
P_1=19,000	1

comparison to the theoretical Milankovitch ratios allows us to interpret peaks at 0.449–0.422 (2.23–2.37 m) with ratios 1: 1.06 as two peaks closed to P_1, peaks at 0.386–0.347 (2.59–2.89 m) with ratios 1.16: 1.29 as two peaks closed to P_2, peaks at 0.198–0.188 (5.05–5.32 m) with ratios at 2.26: 2.39 as two peaks closed to O_1 and the peak at 0.129 (7.77 m) with ratio at 3.48 as O+P. The rest of the peaks, such as that at 0.102 (9.85 m) with ratio at 4.40 and those at 0.0594–0.0495–0.0293 (16.83–20.20–34.13 m) with ratios 7.56: 9.07: 15.3, are registered at frequencies in the eccentricity range but without giving a precise value. According to option A, the registered peaks could be more easily assigned to the high-frequency band, with the record of precession (P_1–P_2) and obliquity (O_1), while the lower frequency band would be represented comparatively worse.

– Option B: As previously mentioned, sampling procedure could determine the comparatively poor record of the high-frequency Milankovitch band cycles in our study, being the best recorded cycles, and then, with a better correspondence with the Milankovitch cycles, those in the lower frequencies. Thus, in option B, we consider that peaks registered in the lowest frequencies, those at 0.0293 (34.13 m), could correspond to the long-term eccentricity E_3, assigning it a theoretical ratio of 21.74 and then recalculate the rest of the ratios. For the registered peaks at 0.0293–0.0495–0.0594 (34.13–20.20–16.83 m), 0.102–0.129 (9.85–7.77 m), 0.188–0.198 (5.32–5.05 m), 0.347–0.386 (2.89–2.59 m), and 0.422–0.449 (2.37–2.23 m), the ratios will be 21.74:12.87:10.72:6.27:4.95: 3.39:3.21:1.84:1.65:1.51:1.42 (Table 4). According to these ratios, the registered peak at 0.0293 will correspond to E_3, those at 0.102–0.129 to E_2–E_1, peaks at 0.188–0.198 as O+P, that at 0.347 to O_1 and that at 0.449 at around P_2. From the rest of the peaks, those at 0.0495–0.0594 could reflect the interaction of the short- and long-term eccentricity. Option B favours the interpretation of a better record with regard to the lower frequency cycles, eccentricity and obliquity against the peaks from the higher frequencies (precession). However, the existence of the precession input is characterized by those peaks related to the combined effect of precession and obliquity.To support one of the two options, the second method can be used, the temporal calibration of the registered peaks.

(2) Considering this sedimentation rate (8.3 cm/ka), the registered peaks could be calibrated as follows (Table 5); peaks at the highest frequencies of 0.422–0.449 (2.37–2.23 m) would represent a duration between 28.44 and 26.76 kyr; those of 0.347–0.386 (2.89–2.59 m) will correspond to 34.68–31.08 kyr; peak at 0.188–0.198 (5.32–5.05 m) will be calibrated as 63.8–60.6 kyr; those at 0.102–0.129 (9.85–7.77 m) will be assigned a duration of 118.2–93.2 kyr;

Table 4
Ratios between the registered peaks in the studied section according to the two options proposed (see text for explanation)

		Option A		Option B	
		Ratios	Interpretation	Ratios	Interpretation
Frequency	Thickness				
0.0293	34.13	15.3	¿?	21.74	E_3
0.0495	20.20	9.07	¿?	12.87	
0.0594	16.83	7.56	¿?	10.72	
0.102	9.85	4.40	¿?	6.27	E_2
0.129	7.77	3.48	O+P	4.95	E_1
0.188	5.32	2.39	O_1	3.39	O+P
0.198	5.05	2.26	O_1	3.21	O+P
0.347	2.89	1.29	P_2	1.84	O_1
0.386	2.59	1.16	P_2	1.65	¿?
0.422	2.37	1.06	P_1	1.51	¿?
0.449	2.23	1	P_1	1.42	P2

Table 5
Periodicity of the selected peaks registered in the spectral analyses of the two selected groups, and interpretation

Frequency	Thickness	Period	Interpretation
0.0293	34.13	409.560	Eccentricity E_3
0.0495	20.20	242.400	
0.0594	16.83	201.960	
0.1016	9.85	118.200	Eccentricity E_2
0.1288	7.77	93.240	Eccentricity E_1
0.1881	5.32	63.840	Precession+obliquity
0.1980	5.05	60.600	Precession+obliquity
0.3465	2.89	34.680	Obliquity O_1
0.3861	2.59	31.080	
0.4219	2.37	28.440	Precession
0.4492	2.23	26.760	Precession

and finally, those peaks at 0.0293–0.0495–0.0594 (34.13–20.20–16.83 m) a duration of 411–243–202 kyr. According to this, we could interpret the record of (a) a poorly represented precession cycle due to the fact that the extreme is around 28 kyr, (b) the obliquity cycle near O_1, and (c) the short- and long-term eccentricity interact with favouring cycles at intermediate frequencies. The peaks around 64–61 ka could be interpreted as the combined effect of precession and obliquity.

From the above, the most plausible interpretation could be that considering option B, similar to that determined by the temporal calibration of the registered peaks.

- In the range of the lower frequencies, extreme peaks at 0.0293 (34.13 m) can be correlated with the long-term eccentricity (ratio of 21.74), with a duration of 410 ka. Peaks at 0.102–0.129 (9.85–7.77 m), with ratios of 6.27 and 4.95, may correspond to the short-term eccentricity, with a duration of 118–93 ka. Peaks at 0.0495–0.0594 (20.20–16.83 m), with ratios of 12.87 and 10.72, could correspond to the interaction between the peaks assigned to the long- and short-term eccentricity.
- In the range of intermediate frequencies, peaks at 0.188–0.198 (5.32–5.05 m), with ratios of 3.39–3.21, and calibrated as 63,840–60,600 years, fit well with peaks assigned to the combined effect of precession and obliquity.
- In the range of high frequencies, peaks at 0.347–0.386 (2.89–2.59 m), with ratios of 1.84 and 1.65, and periods of 34,680–31,080 years, are interpreted as the record of the obliquity cycle (around 31,000 in Berger, 1977). Peaks registered at the highest frequencies of 0.422–0.449 (2.37–2.23 m), with ratios of 1.51–1.42, and periods between 28,440–26,760 years could be tentatively assigned to some components of the precession, but resolution of the sampling procedure could influence its record.

The interpretation reached is in accordance with previous analyses on Milankovitch cyclicity during the early and middle Miocene. During the Oligocene/Miocene boundary and the early and mid-Miocene, Milankovitch forcing shows the dominance of the obliquity cycle with a period of about 41,000 years and, secondarily, the eccentricity cycles around 400,000 and 100,000 years, while the record of the precession cycle is difficult to detect (Flower et al., 1997; Shackleton and Crowhurst, 1997; Weedon and Shackleton, 1997; Shackleton et al., 1999, 2000; Abdul Aziz et al., 2000; Paul et al., 2000; Naish et al., 2001; Zachos et al., 2001a,b; Hall et al., 2003; Holbourn et al., 2003; Rocca et al., 2003; Weedon, 2003). Spectral analyses in marine sequences from the Western Equatorial Atlantic (Flower et al., 1997; Weedon and Shackleton, 1997; Paul et al., 2000), Indopacific region (Hall et al., 2003) and Antarctic Continental Margin (Naish et al., 2001) confirm concentrations of variance at 400-, 100- and 41-kyr periods, suggesting a high-latitude control on climatic variability, probably related to the Southern Component Water (SCW) and the East Antarctic Ice Sheet (EAIS) variability. Far from these regions, Milankovitch control on deep water during the middle Miocene has also been interpreted for comparatively smaller depositional areas, as the Tethys region (Rocca et al., 2003).

Thus, the weak record of the precession signals in our spectral section could be a consequence of the sampling procedure or of the particular Milankovitch dominance during this time, the eccentricity and mainly the obliquity cycles being better characterized. However, in our case study, working on pollen data deposited in a comparatively small and isolated area, the incidence of oceanographic processes determining

the cyclic variations registered in the time series can be secondary. Regarding the interpretation of fluctuations in vegetation components sensitive to climatic changes, the different response to orbital forcing has been related to a variable incidence on climatic components (i.e., precipitation, temperature; Mommersteeg et al., 1995; Okuda et al., 2002; Popescu, 2001). Time series of pollen data showing a precession and obliquity signals were related to changes in net precipitation (Mommersteeg et al., 1995), while cycles in the range of the eccentricity band were related to changes in temperature (Mommersteeg et al., 1995; Popescu, 2001). Periodic changes in the distribution (expansion) of vegetation forced by astronomical cycles could determine fluctuations in pollen abundance from the different groups. Fluctuations in annual rainfall induced by precession forcing were interpreted as responsible for changes in input of freshwater and then terrigenous to the basin at the time of Mediterranean sapropels formation during the late Miocene (Veen and Postma, 1996; Sierro et al., 2000).

5.3. Eustatic changes

Some eustatic changes can be interpreted through time. Significant changes observed in percentages of *Pinus* and indeterminable Pinaceae (Fig. 8) could have been produced, as seen in modern pollen sedimentation, by eustatic changes due to the efficiency in the transport of these pollen grains (Suc and Drivaliari, 1991; Cambon et al., 1997). Therefore, the percentage of these bisaccate pollen grains increases with the distance to the coast line (Turon, 1984; Heusser, 1988; Cambon et al., 1997). Dinoflagellate cysts confirm this supposition. The abundance of characteristic dinocysts of open marine environments reveals that marine conditions have prevailed since the Karpatian (Fig. 8). During the Sarmatian, this area was characterized by a very shallow sea in which any change could alter water conditions, such as salinity, paleodepth, etc. Therefore, several marine organisms vanished during that time (Bohn-Havas, 1982; Nagymarosi, 1982). Dinoflagellate cysts were also very affected by this regression and this new unstable marine condition characterized principally by a decrease in salinity of the marine waters due to more fresh water influx.

A regression from marine to continental conditions is supposed to have taken place in the Karpatian/Badenian and at the Badenian/Sarmatian boundaries, when there was a lack of dinocysts and an important decrease in the percentage of *Pinus* and indeterminable Pinaceae. Both clear regressions are third-order depositional sequence boundaries; the Bur-5/Lan-1 (Karpatian/Badenian) and Ser-1 (Badenian/Sarmatian) from Vakarcs et al. (1998). The deposition, during the Badenian/Sarmatian boundary, of continental sediments is consistent with the presence in this boundary (723.1 m) of the continental gastropod *Archeozonites* sp. (Bohn-Havas, 1982) and the existence of erosion (Kókay, 1996).

As we have seen before, a decrease in floral diversity and thermophilous elements along the Badenian and in the Sarmatian has also been observed correlated with the increase in development of the EAIS. Therefore, the climatic cooling (see Fig. 5) could explain the Ser-1/Ser-2 regression. This is in agreement with the data of Vakarcs et al. (1998) and Báldi et al. (2002) for these two boundaries. They show that the short-term glacio-eustatic falls can be correlated with regional stage boundaries and overprint long-term local tectonics which are two phases that resulted in second-order transgressive/regressive cycles. Báldi et al. (2002), who provided the subsidence history of the Tengelic 2 borehole, explained the Early–Late Badenian regression (Lan-2/Ser-1) as a significant uplift which produced a shallowing of the basin. In our palynological study, this sequence boundary has not been fully appreciated as complete marine conditions remained during this regression.

6. Conclusions

Palynological analysis of the Karpatian–Sarmatian part of the borehole Tengelic 2 (Pannonian Basin, Hungary) allowed us to recreate the vegetation and its organization, palaeoecology and climate during the middle Miocene in the Paratethys area. In addition, stratigraphical changes, together with pollen and dinocysts information, permitted us to reconstruct eustatic fluctuations.

The presented data on pollen suggest a forest organized in altitudinal belts comparable to the one now existing in southeastern China (Wang, 1961; Axelrod et al., 1996). Thus, a subtropical–warm temperate humid climate is inferred.

Karpatian and Early Badenian floras reflect the Miocene climatic optimum (MCO) as they are extremely rich in thermophilous elements. Immediately following, a progressive decrease in thermophilous elements and floral diversity occurred during the Late Badenian and Sarmatian. This is consistent with the estimated values of temperature and precipitation using the pollen data from the "climatic amplitude method." A decrease in mean annual temperature (Ta) of about 18–20 °C during the Badenian to ca. 16 °C in the Sarmatian, and a decrease in mean annual precipitation (Pa) of about 1200–1400 mm during the Badenian to 1100 mm during the Sarmatian is seen. This has been interpreted as a climatic cooling during the "Monterey Cooling Event," correlated with the increase in development of the East Antarctic Ice Sheet (EAIS). This trend of cooling is also accompanied here by a decrease in precipitation.

The Late Badenian stage is characterized in this borehole by repetitive changes in vegetation characterized by the alternation of thermophilous and hygrophilous taxa with altitudinal and xerophilous taxa. The astronomical tuning of these vegetation changes to the eccentricity and insolation time series of the $La93_{(1,1)}$ solution is rather consistent. Spectral analysis of pollen data reveals the influence of astronomical climatic changes (Milankovitch scale) on the evolution of the studied vegetation. Obliquity and eccentricity (short and long term) cycles are dominant, while precession influence is poorly registered. Combination of pollen data and dinocysts information allowed us to appreciate and characterize eustatic changes in this study. The Ser-2 sequence boundary (Vakarcs et al., 1998) here is clearly related to this climatic cooling.

Acknowledgments

We would like to thank Laszló Kordos for the permission of sampling the Tengelic-2 borehole, Mária Sütóné Szentai, Speranta-Maria Popescu, A. Dulai and Derzsó Illés who kindly helped us out with the sampling. Graham P. Weedon is thanked for improving the manuscript. We would also like to thank Jodi Eckart for the English corrections. G.J.-M.'s research is funded by a PhD grant from the "Junta de Andalucía" (Spain). F.J.R.-T was supported by Projects REN2000-0798 and BTE2001-3029 (DGICYT) and the Group RNM-178 (Junta de Andalucía) and by the French Ministry of Research (cotutelle grant). Trips to Hungary for sampling have been supported by CNRS and the Hungarian Academy of Sciences within the frame of a cooperative project (leaders: P. Moissette and A. Dulai). Three of the authors (G.J.-M., S.F. and J.-P.S.) are indebted to the EEDEN Programme (ESF) for invitations to participate to several international workshops. This is an ISEM contribution 2004-075.

References

Abdul Aziz, H., Hilgen, F., Krijgsman, W., Sanz, E., Calvo, J.P., 2000. Astronomical forcing of sedimentary cycles in the middle to late Miocene continental Calatayud Basin (NE Spain). Earth Planet. Sci. Lett. 177, 9–22.

Andreanszky, G., 1959. Die Flora der Sarmatischen Stufe in Ungarn. Akadémiai Kiadó, Budapest.

Axelrod, D.I., Al-Shehbaz, I., Raven, P., 1996. History of the modern flora of China. In: Aoluo, Z., Sugong, W. (Eds.), Floristic Characteristics and Diversity of East Asian Plants. Springer-Verlag, Berlin, pp. 43–55.

Báldi, K., Benkovics, L., Sztanó, O., 2002. Badenian (middle Miocene) basin development in SW Hungary: subsidence history based on quantitative paleobathymetry of foraminifera. Int. J. Earth Sci. 91, 490–504.

Barrón, E., 1999. Estudio palinológico de la cuenca miocena de Rubielos de Mora (Teruel, España). Aspectos paleoecológicos y paleobiogeográficos. Bol. R. Soc. Esp. Hist. Nat., Secc. Geol. 95 (1–4), 67–82.

Beaudouin, C., 2003. Effets du dernier cycle climatique sur la vegetation de la basse vallée du Rhône et sur la sédimentation de la plate-forme du golfe du Lion d'après la palynologie. Ph.D. thesis, Univ. C. Bernard-Lyon 1, France, 403 p.

Berger, A.L., 1977. Support for the astronomical theory of climatic change. Nature 269, 44–45.

Berger, A., Loutre, M.F., Dehant, V., 1989. Milankovitch frequencies for pre-Quaternary. Nature 342, 133.

Berger, A., Loutre, M.F., Laskar, J., 1992. Stability of the astronomical frequencies over the Earth's history for paleoclimate studies. Science 255, 560–566.

Berggren, W.A., Kent, D.V., Swisher, C.C., Aubry, M.P., 1995. A revised Cenozoic geochronology and chronostratigraphy. In: Berggren, W.A., Kent, D.V., Aubry, M.-P., Hardenbol, J. (Eds.), Geochronology, Time Scales and Global Stratigraphic Correlations, SEPM, Spec. Publ., vol. 54, pp. 129–212 (Tulsa).

Bertini, A., 1994. Messinian–Zanclean vegetation and climate in north-central Italy. Hist. Biol. 9, 3–10.

Bertini, A., Londeix, L., Maniscalco, R., Di Stefano, A., Suc, J.-P., Clauzon, G., Gautier, F., Grasso, M., 1998. Paleobiological evidence of depositional conditions in the salt member, Gessoso–Solfifera Formation (Messinian, upper Miocene) of Sicily. Micropaleontology 44 (4), 413–433.

Bessedik, M., 1985. Reconstitution des environnements Miocènes des régions nord-ouest Mediterraneénnes à partir de la palynologie. PhD thesis, Univ. Sciences et Techniques du Languedoc, Montpellier, France.

Bohn-Havas, M., 1982. Mollusca fauna of Badenian and Sarmatian stage from the borehole Tengelic 2. In: Nagy, E., Bodor, E., Hagyamarosi, A., Korecz-Laky, I., Bohn-Havas, M., Sütó-Szentai, M., Széles, M., Korpás-Hódi, M. (Eds.), Palaeontological examination of the geological log of the borehole Tengelic 2, Ann. Geol. Publ. Hung., vol. 65, pp. 200–203 (Budapest).

Cambon, G., Suc, J.-P., Aloisi, J.-C., Giresse, P., Monaco, A., Touzani, A., Duzer, D., Ferrier, J., 1997. Modern pollen deposition in the Rhône delta area (lagoonal and marine sediments) France. Grana 36, 105–113.

Cour, P., 1974. Nouvelles techniques de detection des flux et des retombées polliniques: etude de la sédimentation des pollens et des spores à la surface du sol. Pollen Spores 16 (1), 103–141.

Drivaliari, A., 1993. Images polliniques et paléoenvironnement au Néogène supérieur en Méditerranée orientale. Aspects climatiques et paléogéographiques d'un transect latitudinal (de la Roumanie au Delta du Nil). PhD thesis, Univ. Montpellier-2, France.

Fauquette, S., Bertini, A., 2003. Quantification of the northern Italy Pliocene climate from pollen data—evidence for a very peculiar climate pattern. Boreas 32 (2), 361–369.

Fauquette, S., Guiot, J., Suc, J.-P., 1998a. A method for climatic reconstruction of the Mediterranean Pliocene using pollen data. Palaeogeogr. Palaeoclimatol. Palaeoecol. 144, 183–201.

Fauquette, S., Quézel, P., Guiot, J., Suc, J.-P., 1998b. Signification bioclimatique de taxons-guides du Pliocène Méditerranéen. Géobios 31, 151–169.

Fauquette, S., Suc, J.-P., Guiot, J., Diniz, F., Feddi, N., Zheng, Z., Bessais, E., Drivaliari, A., 1999. Climate and biomes in the west Mediterranean area during the Pliocene. Palaeogeogr. Palaeoclimatol. Palaeoecol. 152, 15–36.

Fauquette, S., Suc, J.-P., Bertini, A., Popescu, S.-M., Warny, S., Bachiri Taoufiq, N., Perez Villa, M.J., Ferrier, J., Chikhi, H., Subally, D., Feddi, N., Clauzon, G., 2004. How much the climate forced the Messinian salinity crisis? Quantified climatic conditions from pollen. Palaeogeogr. Palaeoclimatol. Palaeoecol (in press).

Flower, B., Kennett, J., 1994. The middle Miocene climatic transition: East Antartic Ice Sheet development, deep ocean circulation and global carbon cycling. Palaeogeogr. Palaeoclimatol. Palaeoecol. 108, 537–555.

Flower, B.P., Zachos, J.C., Paul, H., 1997. Milankovitch-scale climate variability recorded near the Oligocene/Miocene boundary. In: Shackleton, N.J., Curry, W.B., Richter, C., Bralower, T.J. (Eds.), Proc. ODP, Scientific Results, vol. 154, pp. 433–439.

Hall, I.A., McCave, N., Zahn, R., Carter, L., Knutz, P.C., Weedon, G.P., 2003. Paleocurrent reconstruction of the deep Pacific inflow during the middle Miocene: reflections of East Antarctic Ice sheet growth. Paleoceanography 18 (2), 1040, 1–11.

Halmai, J., Jámbor, A., Ravasz-Baranyai, L., Vetö, I., 1982. Geological results of the borehole Tengelic-2. Ann. Inst. Geol. Publici Hung. 65, 93–138.

Hámor, G., 1995. Miocene Palaeogeographic and Facies Map of the Carpathian Basin. Eötvös Lorand University, Budapest (Hungary).

Harland, R., 1983. Distribution map of recent dinoflagellate cysts in bottom sediments from the North Atlantic Ocean and adjacent seas. Palaeontology 26, 321–387.

Heusser, L., 1988. Pollen distribution in marine sediments on the continental margin of northern California. Mar. Geol. 80, 131–147.

Holbourn, A., Kuhnt, W., Schulz, M., 2003. Milankovitch forcing and role of Indonesian gateway on middle Miocene climate and carbon cycle: new perspective from the South China Sea, Equatorial West Pacific and East Indian Ocean. Geophys. Res. Abstr. 5, 06151.

Hooghiemstra, H., Agwu, C.O.C., Beug, H.J., 1986. Pollen and spore distribution in recent marine sediments: a record of NW-African seasonal wind patterns and vegetation belts. Meteor-Forsch.Ergeb. 40, 87–135.

Ivanov, D., Ashraf, A.R., Mosbrugger, V., Palmarev, E., 2002. Palynological evidence for Miocene climate change in the Forecarpathian Basin (central Paratethys, NW Bulgaria). Palaeogeogr. Palaeoclimatol. Palaeoecol. 178, 19–37.

Kókay, J., 1996. Stratigraphical analysis of Badenian sections from western Hungary (Transdanubia) compared to the eustatic sea-level changes (in Hungarian, with English abstract). Foldt. Kozlony 126, 97–115.

Korecz-Laky, I., 1982. Miocene foraminifera fauna from the borehole Tengelic 2. In: Nagy, E., Bodor, E., Hagyamarosi, A., Korecz-Laky, I., Bohn-Havas, M., Sütó-Szentai, M., Széles, M., Korpás-Hódi, M. (Eds.), Palaeontological Examination of the Geological Log of the Borehole Tengelic 2, Ann. Inst. Geol. Publici Hung., vol. 65, pp. 186–187 (Budapest).

Laskar, J., 1990. The chaotic motion of the solar system: a numerical estimate of the size of the chaotic zones. Icarus 88 (2), 266–291.

Laskar, J., Joutel, F., Boudin, F., 1993. Orbital, precessional, and insolation quantities for the Earth from −20 Myr to +10 Myr. Astron. Astrophys. 270, 522–533.

Meulenkamp, J.E., Sissingh, W., 2003. Tertiary palaeogeography and tectonostratigraphic evolution of the Northern and Southern Peri-Tethys platforms and the intermediate domains of the African–Eurasian convergent plate boundary zone. Palaeogeogr. Palaeoclimatol. Palaeoecol. 196, 209–228.

Miller, K.G., Feigenson, M., Wright, J.D., Clement, B., 1991. Miocene isotope reference section, Deep Sea Drilling Project Site 608: an evaluation of isotope and biostratigraphic resolution. Paleoceanography 6 (1), 33–52.

Mommersteeg, H.J.P.M., Loutre, M.F., Young, R., Wijmstra, T.A., Hooghiemstra, H., 1995. Orbital forced frequencies in the 975.000 year pollen record from Tenagi Philippon (Greece). Clim. Dyn. 11, 4–24.

Nádor, A., Lantos, M., Tóth-Makk, A., Thamó-Bozsó, E., 2003. Milankovitch-scale multi-proxy records from fluvial sediments of the last 2.6 Ma, Pannonian Basin, Hungary. Quat. Sci. Rev. 22, 2157–2175.

Nagy, E., 1991. Climatic changes in the Hungarian Neogene. Rev. Palaeobot. Palynol. 65 (1–4), 71–74.

Nagy, E., 1992. Magyarorszag Neogen sporomorphainak ertekelese. Geol. Hung. 53, 1–379.

Nagyamarosi, A., 1982. Badenian–Sarmatian nannoflora from the borehole Tengelic 2. In: Nagy, E., Bodor, E., Hagyamarosi, A., Korecz-Laky, I., Bohn-Havas, M., Sütó-Szentai, M., Széles, M., Korpás-Hódi, M. (Eds.), Palaeontological Examination of the Geological Log of the Borehole Tengelic 2, Ann. Inst. Geol. Publici Hung., vol. 65, pp. 145–149 (Budapest).

Naish, T.R., Woolfe, K.J., Barrett, P.J., Wilson, G.S., Atkins, C., Bohaty, S.M., Bücker, C.J., Claps, M., Davey, F.J., Dunbar, G.B., Dunn, A.G., Fielding, C.R., Florindo, F., Hannah, M.J., Harwood, D.M., Henrys, S.A., Krissek, L.A., Lavelle, M., van der Meer, J., McIntosh, W.C., Niessen, F., Passchier, S., Powell, R.D., Roberts, A.P., Sagnotti, L., Scherer, R.P., Strong, C.P., Talarico, F., Verosub, K.L., Villa, G., Watkins, D.K., Webb, P.-N., Wonik, T., 2001. Orbitally induced oscillations in the East Antarctic Ice Sheet at the Oligocene/Miocene boundary. Nature 413, 719–723.

Naud, G., Suc, J.-P., 1975. Contribution à l'étude paléofloristique des Coirons (Ardèche): premières analises polliniques dans les alluvions sous-basaltiques et interbasaltiques de Mirabel (Miocène supérieur). Bull. Soc. Geol. Fr. 7 (5), 820–827.

Okuda, M., van Vugt, N., Nakagawa, T., Ikeya, M., Hayashida, A., Yasuda, Y., Setoguchi, T., 2002. Palynological evidence for the astronomical origin of lignite–detritus sequence in the middle Pleistocene Marathousa Member, Magapolis, SW Greece. Earth Planet. Sci. Lett. 201, 143–157.

Pardo-Igúzquiza, E., Chica-Olmo, M., Rodríguez-Tovar, F.J., 1994. CYSTRATI: a computer program for spectral analysis of stratigraphic successions. Comput. Geosci. 20, 511–584.

Pardo-Igúzquiza, E., Schwarzacher, W., Rodríguez-Tovar, F.J., 2000. A library of computer programs for assisting teaching and research in cyclostratigraphic analysis. Comput. Geosci. 26, 723–740.

Paul, H.A., Zachos, J.C., Flower, B.P., Tripati, A., 2000. Orbitally induced climate and geochemical variability across the Oligocene/Miocene boundary. Paleoceanography 15, 471–485.

Planderová, E., 1990. Miocene Microflora of Slovak central Paratethys and its Biostratigraphical Significance. Dionyz Stur Institute of Geology, Bratislava (Slovakia) (143 pp).

Pons, A., 1964. Contribution palynologique à l′ étude de la flore et de la végétation Pliocènes de la region Rhodanienne. Ann. Sci. Nat., Paris, Bot. 5, 599–722.

Popescu, S.-M., 2001. Repetitive changes in Early Pliocene vegetation revealed by high-resolution pollen analysis: revised cyclostratigraphy of southwestern Romania. Rev. Palaeobot. Palynol. 120 (3–4), 181–202.

Popescu, S.-M., Suc, J.-P., Loutre, M.-F., in press. Early Pliocene vegetation changes forced by eccentricity-precession in southwestern Romania. Palaeogeogr. Palaeoclimatol. Palaeoecol.

Quézel, P., Médail, F., 2003. Ecologie et Biogéographie des Forêts du Bassin Méditerranéen. Elsevier, France (571 pp).

Rivas-Carballo, M.R., 1991. The development of vegetation and climate during the Miocene in the south-eastern sector of the Duero Basin (Spain). Rev. Palaeobot. Palynol. 67, 341–351.

Rocca, D., Bellanca, A., Neri, R., Russo, B., Sgarrella, F., Sprovieri, M., 2003. A Milankovitch climate control on the middle Miocene Mediterranean intermediate water: evidence from benthic microfauna and isotope geochemistry of the Ras Il-Pellegrin composite section (Malta island, Central Mediterranean). Geophys. Res. Abstr. 5, 14359.

Rögl, V.F., 1998. Palaeogeographic considerations for Mediterranean and Paratethys seaways (Oligocene to Miocene). Ann. Naturhist. Mus. Wien 99A, 279–310.

Royden, L.H., Horváth, F., 1988. The Pannonian Basin. A study in basin evolution. Am. Assoc. Pet. Geol. Mem. 45 (394 pp).

Saint Martin, J.-P., Müller, P., Moissette, P., Dulai, A., 2000. Coral microbialite environment in a middle Miocene reef of Hungary. Palaeogeogr. Palaeoclimatol. Palaeoecol. 160, 179–191.

Schwarzacher, W., 1975. Sedimentation Models and Quantitative Stratigraphy, Developments in Sedimentology, vol. 19. Elsevier, Amsterdam (382 pp).

Schwarzacher, W., 1993. Cyclostratigraphy and the Milankovitch Theory, Developments in Sedimentology, vol. 52. Elsevier, Amsterdam (225 pp).

Shackleton, N.J., Crowhurst, S., 1997. Sediment fluxes based on an orbitally tuned time scale 5 Ma to 14 Ma, site 926. In: Shackleton, N.J., Curry, W.B., Richter, C., Bralower, T.J.Proc. ODP, Scientific Results, vol. 154, pp. 69–82.

Shackleton, N.J., Crowhurst, S.J., Weedon, G.P., Laskar, J., 1999. Astronomical calibration of Oligocene–Miocene time. Philos. Trans. R. Soc. Lond., A 357, 1907–1929.

Shackleton, N.J., Hall, M.A., Raffi, I., Tauxe, L., Zachos, J., 2000. Astronomical calibration age for the Oligocene–Miocene boundary. Geology 28, 447–450.

Sierro, F.J., Ledesma, S., Flores, J.A., Torrescusa, S., Martínez del Olmo, W., 2000. Sonic and gamma-ray astrochronology: cycle to cycle calibration of Atlantic climatic records to Mediterranean sapropels and astronomical oscillations. Geology 28, 695–698.

Steininger, F., 1999. Chronostratigraphy, geochronology and biochoronology of the Miocene "European land mammal megazones" (ELMMZ) and the Miocene "mammal-zones (MN-Zones). In: R"ssner, G.E., Heissig, K. (Eds.), The Miocene Land Mammals of Europe. Verlag, Münich, pp. 9–24.

Steininger, F.F., Bernor, R.C., Fahlbusch, V., 1990. European Neogene marine/continental chronologic correlations. In: Lindsay, E.H., Fahlbusch, V., Mein, P. (Eds.), European Neogene Mammals Chronology. Plenum Press, New York, pp. 15–46.

Steininger, F.F., Berggren, W.A., Kent, D.V., Bernor, R.L., Sen, S., Agustí, J., 1996. Circum–Mediterranean Neogene (Miocene and Pliocene) marine–continental chronologic correlations of European mammal units. In: Bernor, R.L., Fahlbusch, V., Mittmann, H.-W. (Eds.), The Evolution of Western Eurasian Neogene Mammal Faunas. Columbia University Press, New York, pp. 7–23.

Suc, J.-P., 1976. Quelques taxons-guides dans l'étude paléoclimatique du Pliocène et du Pleistocène infèrieur du languedoc (France). Rev. Micropaleontol. 18 (4), 246–252.

Suc, J.-P., 1984. Origin and evolution of the Mediterranean vegetation and climate in Europe. Nature 307, 429–432.

Suc, J.-P., Bessedik, M., 1981. Methodology for Neogene palynostratigraphy. In: Martinell, J. (Ed.), Concept and Method in Paleontology, Barcelona, pp. 205–208.

Suc, J.-P., Drivaliari, A., 1991. Transport of bisaccate coniferous fossil pollen grains to coastal sediments: an example from the earliest Pliocene Orb Ria (Languedoc, Southern France). Rev. Palaeobot. Palynol. 70, 247–253.

Tari, G., 1992. Late Neogene transgression in the northern trust zone Mecsek Mts, Hungary, Ann. Eötvös University Budapest. Sect. Geol. 29, 165–187.

Thomson, D.J., 1982. Spectrum estimation and harmonic analysis. Proc. IEEE 70, 1055–1096.

Turon, J.-L., 1984. Le palynoplacton dans l'environnement actuel de l'Atlantique nord-oriental. Evolution climatique et hydrobiologique depuis le dernier maximum glaciaire, PhD thesis, Univ. Bordeaux-1, Bordeaux, France.

Vakarcs, G., Handerbol, J., Abreu, V.S., Vail, P., Várnai, P., Tari, G., 1998. Oligocene–Middle Miocene depositional sequences of the central Paratethys and their correlation with regional stages. In: Gracinssky, P.-C. de, Hardenbol, J., Jacquin, T., Vail, P.R. (Eds.), Mesozoic and Cenozoic Sequence Stratigraphy of European Basins, SEPM, Spec. Publ., vol. 60, pp. 209–231 (Tulsa).

Valle, M.F., Alonso Gavilán, G., Rivas-Carballo, M.R., 1995. Analyse Palynologique Préliminare du Miocène dans le NE de la Dépresision du Duero (aire de Belorado, Burgos, España). Géobios 28 (4), 407–412.

Veen, J.H. ten, Postma, G., 1996. Astronomically forced variations in gamma-ray intensity: late Miocene hemipelagic successions in the eastern Mediterranean basin as a test case. Geology 24, 15–18.

Wall, D., Dale, B., Lohmann, G.P., Smith, W.K., 1977. The environmental and climatic distribution of dinoflagellate cysts in modern marine sediments from regions in the north and south Atlantic adjacent seas. Mar. Micropaleontol. 2, 121–200.

Wang, C.W., 1961. The forests of China with a survey of grassland and desert vegetation. Maria Moors Cabot Fundation, vol. 5. Harvard University, Cambridge, Massachussets.

Weedon, G.P., 2003. Time-Series Analysis and Cyclostratigraphy. Cambridge University Press, New York (259 pp).

Weedon, G.P., Shackleton, N.J., 1997. Inorganic geochemical composition of Oligocene to Miocene sediments and productivity variations in the Western equatorial Atlantic: results from sites 926 and 929. Proc. Ocean Drill. Program Sci. Results 154, 507–526.

Zachos, J., Pagani, M., Sloan, L., Thomas, E., Billups, K., 2001a. Trends, rhythms, and aberrations in global climate 65 Ma to present. Science 292, 686–693.

Zachos, J.C., Schackleton, N.J., Revenaugh, J.S., Pälike, H., Flower, B.P., 2001b. Climate response to orbital forcing across the Oligocene–Miocene boundary. Science 292, 274–278.

Zagwijn, W.H., 1960. Aspects of the Pliocene and Early Pleistocene vegetation in the Netherlands. Meded. Geol. Stich. C 3 (5), 1–78.

Zheng, Z., 1990. Végétations et climats néogènes des Alpes maritimes franco-italiennes d'après les données de l'analyse palynologique. Paleobiol. Cont. 17, 217–244.